NASA Reference Publication 1175

April 1987

Airborne Lidar Measurements of El Chichon Stratospheric Aerosols

January 1984

M. Patrick McCormick
and M. T. Osborn

NASA

NASA Reference Publication 1175

1987

Airborne Lidar Measurements of El Chichon Stratospheric Aerosols

January 1984

M. Patrick McCormick
Langley Research Center
Hampton, Virginia

M. T. Osborn
ST Systems Corporation (STX)
Hampton, Virginia

National Aeronautics
and Space Administration

Scientific and Technical Information Branch

Preface

This is the fifth in a series of reports presenting results from five extensive lidar flight missions. One of the primary purposes of these missions was to determine the spatial distribution and aerosol characteristics of the El Chichon-produced stratospheric material. This particular mission covered latitudes between 38°N and 77°N in January 1984. Results from the first mission, which covered 42°N to 12°N, were reported in NASA Reference Publication 1166 entitled "Airborne Lidar Measurements of El Chichon Stratospheric Aerosols—July 1982." Results from the second mission, which covered 46°N to 46°S during October–November 1982, were reported in NASA Reference Publication 1136; results from the third mission, which covered 27°N to 76°N during January–February 1983, were reported in NASA Reference Publication 1148; and results from the fourth mission, which covered 72°N to 56°S in May 1983, were reported in NASA Reference Publication 1172.

This report contains representative profiles of lidar backscatter ratio, a plot of integrated backscattering values versus latitude, and contours of backscatter mixing ratio versus altitude and latitude. In addition, tables containing numerical values of the backscatter ratio and backscattering function versus altitude are supplied for each profile. This report is intended to give the results of the mission in a ready-to-use format, and no attempt has been made to provide any scientific analysis with the data.

The authors recognize the airborne lidar team of W. H. Fuller, Jr., and B. R. Rouse of the NASA Langley Research Center and W. H. Hunt and F. C. Diehl of Wyle Laboratories, whose dedicated efforts provided these data, and wish to thank the crew and supporting personnel at the NASA Wallops Flight Facility for providing excellent research airplane platforms for conducting these measurements. In addition, thanks go to the many groups at the Canadian and Greenland air bases that provided logistics support during this mission. Finally, the authors wish to express their appreciation to D. J. Hofmann and his group at the University of Wyoming for providing the dustsonde data.

Contents

Summary

This report presents lidar data taken between 38°N and 77°N from a flight mission in January 1984. One of the primary purposes of this mission was to determine the spatial distribution and aerosol characteristics of the El Chichon-produced stratospheric material. Representative profiles of lidar backscatter ratio, plots of integrated backscattering values versus latitude, and contours of backscattering mixing ratio versus altitude and latitude are presented. In addition, tables containing numerical values of the backscatter ratio and backscattering function versus altitude are supplied for each profile. The most massive portion of the material produced by the El Chichon eruptions of late March–early April 1982, which was measured by this flight, resided north of 55°N and was concentrated below 17 km in a layer that peaked at 13 to 15 km. In this latitude region, peak backscatter ratios at a wavelength of 0.6943 μm were approximately 3 and peak integrated backscattering was about 15×10^{-4} sr^{-1}, corresponding to a peak optical depth of approximately 0.07. No attempt has been made in this report to give any detailed explanations or interpretations of the data. This report provides, in a ready-to-use format, the results of this mission to be used in atmospheric and climatic studies.

Introduction

The late March–early April 1982 eruptions of El Chichon in Mexico (17.3°N, 93.2°W) produced the largest enhancements of stratospheric aerosols in at least 20 years. Because of the effects of the eruption cloud from El Chichon and the need for characterizing the cloud spatially, a series of experimental survey flights was carried out to map its latitudinal and vertical distributions. Previous flights in July 1982 (ref. 1), October to November 1982 (ref. 2), January to February 1983 (ref. 3), and May 1983 (ref. 4) provided valuable information on the changes in spatial distribution and optical properties of the El Chichon aerosol over those periods of time. A primary purpose of the January 1984 flight mission was to continue the time base of information on the volcanic aerosol injected by the eruption of El Chichon. This mission had two additional objectives: to assist with the SAM II (Stratospheric Aerosol Measurement II) (ref. 5) satellite correlative measurement program, and if possible, to locate and study the scattering characteristics of polar stratospheric clouds. To accomplish these goals, a NASA Electra airplane, outfitted with a lidar system, was flown during the period from January 19 to January 28, 1984, between latitudes of 38°N and 90°N. To assist with the execution of this mission, the SAM II data were made available in real time (approximately 12 hours delay), and a "quick-look" analysis was carried out. Meteorological data from the National Meteorological Center (NMC) of the National Oceanic and Atmospheric Administration (NOAA) were provided to assist with locating cold stratospheric temperatures where polar stratospheric clouds were most likely to exist. In this way, the airborne lidar could be directed to these locations.

The mission was successful in accomplishing all three of its goals. This report presents the results of the lidar stratospheric measurements taken during flight legs south of Thule, Greenland (76.5°N, 68.7°W). The mission was successful in locating polar stratospheric clouds on three separate flights north of Thule. The results of these measurements are reported by McCormick et al. (ref. 6) and Kent et al. (ref. 7).

Airborne Lidar System

The airborne lidar system used for the measurements presented in this report consists of a ruby laser, nominally emitting 1 joule per pulse at 1 pulse per 2 seconds at a wavelength (λ) of 0.6943 μm during flight, and a 35.6-cm cassegrainian-configured receiving telescope. Two photomultipliers, electronically switched on at specific times after laser firing, are used to enhance dynamic range. The photomultiplier output signals are processed with an analog-to-digital converter and microprocessor computer, stored on magnetic tape, and displayed on an interactive terminal. The transmitted output divergence is 1.0 mrad, and the receiver field-of-view is 2.0 mrad. Two 40.6-cm quartz windows separated by 1 m are used in the top of the fuselage of the airplane. One window is used for the laser transmitter, and the other, for the telescope receiver. The signal becomes usable at 3 to 4 km above the altitude of the airplane. A detailed error analysis for this system is described by Russell et al. (ref. 8).

Flight Path

The flight path for the January 1984 mission is given in figure 1. The northbound and southbound flight legs are represented by solid lines and dashed lines, respectively. As expected, overlying upper tropospheric clouds prevented measurements at some latitudes, but a remarkable amount of high-quality data were successfully recorded at most latitudes. Table A1 (in the appendix) contains an abbreviated

flight log for the mission and lists the date, time, location, and flight altitude for those legs of the mission in which good-quality lidar data were obtained.

Lidar Profiles

The lidar backscatter ratio (or scattering ratio) is defined as

$$R(z) = 1 + \frac{f_A(z)}{f_M(z)} \quad (1)$$

where f_A is the aerosol backscattering function, or scattering function, and f_M is the molecular backscattering function, both in units of $(\text{km-sr})^{-1}$ and both at altitude z (ref. 9). Representative vertical profiles of lidar scattering ratio for the flight survey are shown in figures 2 to 15. The error bars reflect the 1 - σ uncertainty in the derived scattering ratio. The tropopause height is indicated by an arrow. Tables A2 to A15 (in the appendix) contain numerical values of the aerosol scattering ratio and scattering function versus altitude for each of these profiles.

The scattering-ratio profiles, reported at 0.15-km intervals, have been smoothed over 0.3 km. The minimum three-point running average over a specified altitude range was computed for each profile. The profiles were then normalized so that this minimum was 1, a value that would be obtained only if no aerosols were present at some altitude within the normalization region. Occasionally, the numerical values of the scattering ratio are less than 1, and the corresponding scattering functions are negative. This occurs near the normalization height and when the profile contains minima outside the normalization region. Minimum values of the scattering ratio and scattering function should be considered 1 and 0, respectively.

As shown in figures 2 to 15, material produced by the El Chichon eruptions had spread throughout the latitudes between 38°N and 77°N. Peak backscatter ratio values at $\lambda = 0.6943$ μm varied from 1.8 at 40°N to approximately 3 north of 58°N. The altitude of the peak backscatter ratio decreased with increasing latitude from 17 km at 40°N to 13 km at 70°N.

Integrated Backscattering

The integrated aerosol backscattering function is defined as

$$\int_{h_T}^{28\ \text{km}} f_A(z)\, dz \quad (2)$$

where f_A is the aerosol backscattering function $(\text{km-sr})^{-1}$ at altitude z, and h_T is the height of the tropopause at the location where the lidar data were taken. The integrated aerosol backscattering function for all usable lidar data from the January 1984 mission, except for the three flight legs north of Thule, was combined and averaged into 2.5° latitude bins and is plotted in figure 16. Figure 16 shows that the peak of the material produced by the El Chichon eruptions of late March–early April 1982 had moved northward since January–February 1983 (ref. 3). By January 1984, the most massive portion resided north of 55°N with the peak amount of 15×10^{-4} sr^{-1} occurring near 60°N.

Contours of Backscatter Mixing Ratio

The backscatter mixing ratio is defined as f_A/f_M, or $R(z) - 1$. The symbol $R(z)$ was defined previously in equation (1). Contours of backscatter mixing ratio were plotted for all the southbound and northbound lidar data to determine the vertical as well as the latitudinal distribution of the El Chichon-produced aerosol. Figure 17 contains both the northbound and southbound contours. These contour plots clearly show that the altitude of the peak mixing ratio decreases with increasing latitude. At latitudes north of 55°N, the bulk of the material is shown to reside below 17 km.

Optical Depth and Mass

By using the size distribution from a six-channel dustsonde launch on December 21, 1983, from Laramie, Wyoming (41°N), an aerosol optical model was constructed. The model gives a conversion value from integrated backscattering to column density of 21.3 g-sr/m^2 (ref. 10).

Similarly, by using the aerosol characteristics determined from the dustsonde flight as representative of the aerosol over the most massive part of the stratospheric cloud, the value for converting integrated backscattering to optical depth was calculated to be 47.5 sr. Peak optical depth values of about 0.07 at $\lambda = 0.6943$ μm were thus determined near 60°N.

Concluding Remarks

This report has presented a summary of the lidar data obtained during the January 1984 flight mission to the Arctic region. One purpose of this mission was to determine the spatial distribution and aerosol characteristics of the El Chichon-produced stratospheric material. Vertical profiles of aerosol backscatter ratio were determined which showed that material produced by the El Chichon eruptions of

late March–early April 1982 had spread throughout the latitudes from 38°N to 77°N. Peak backscatter ratios at a wavelength of 0.6943 μm varied from 1.8 at 40°N to approximately 3 north of 58°N. The altitude of the peak backscatter ratio decreased with increasing latitude from 17 km at 40°N to 13 km at 70°N. A plot of integrated backscattering values versus latitude shows that the most massive portion of the cloud produced by El Chichon, which was measured by this flight mission, resided north of 55°N. Peak integrated backscattering was about 15×10^{-4} sr^{-1}, corresponding to a peak optical depth of approximately 0.07. Contours of backscatter mixing ratio versus altitude and latitude further describe the latitudinal and vertical distribution of the El Chichon aerosol. In addition, tables containing numerical values of the backscatter ratio and backscattering function versus altitude have been supplied for each profile. Thus, the lidar data from the mission have been presented in a ready-to-use format for further scientific analysis.

NASA Langley Research Center
Hampton, VA 23665-5225
February 6, 1987

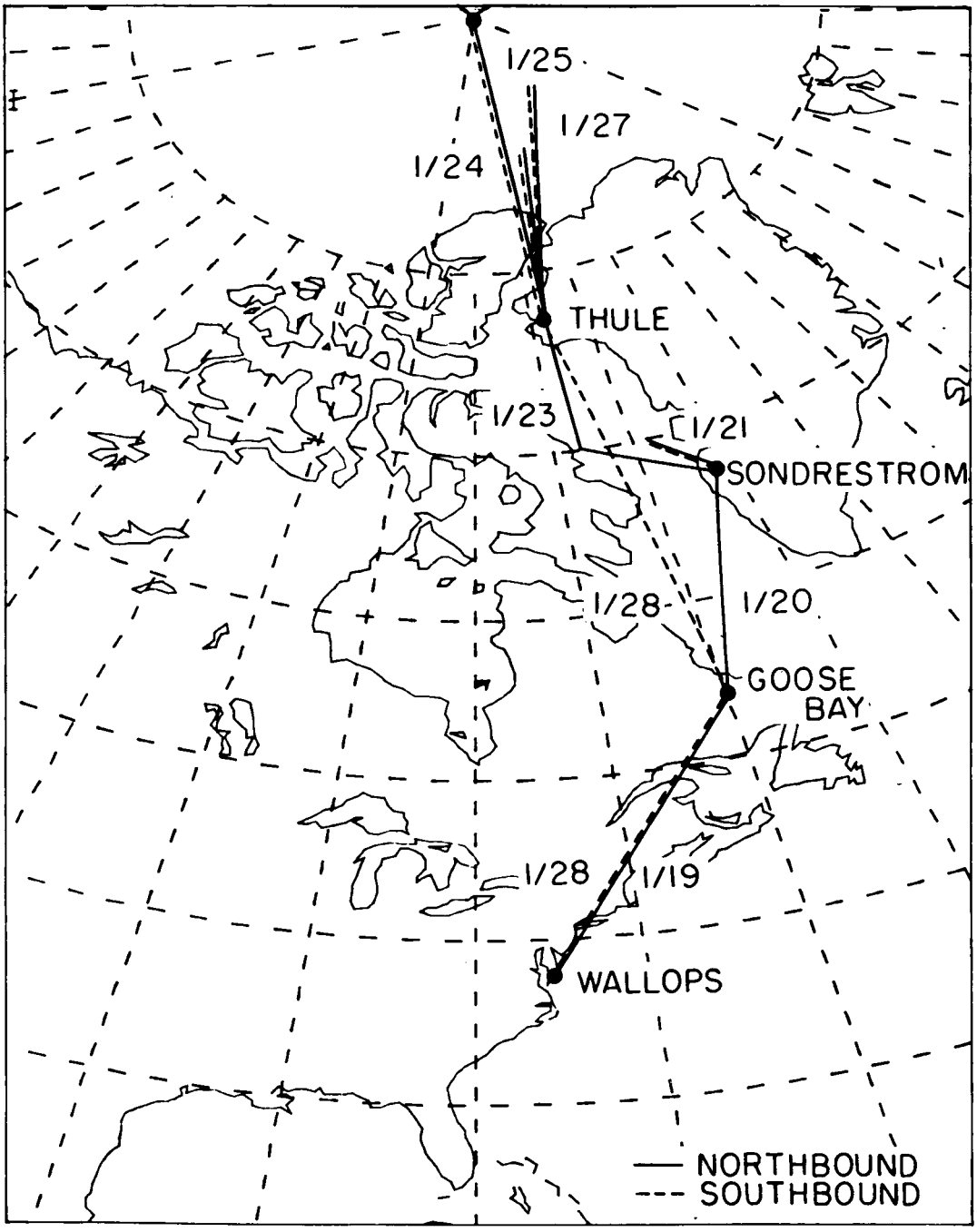

Figure 1. Flight path of NASA Electra airplane from January 19 to January 28, 1984.

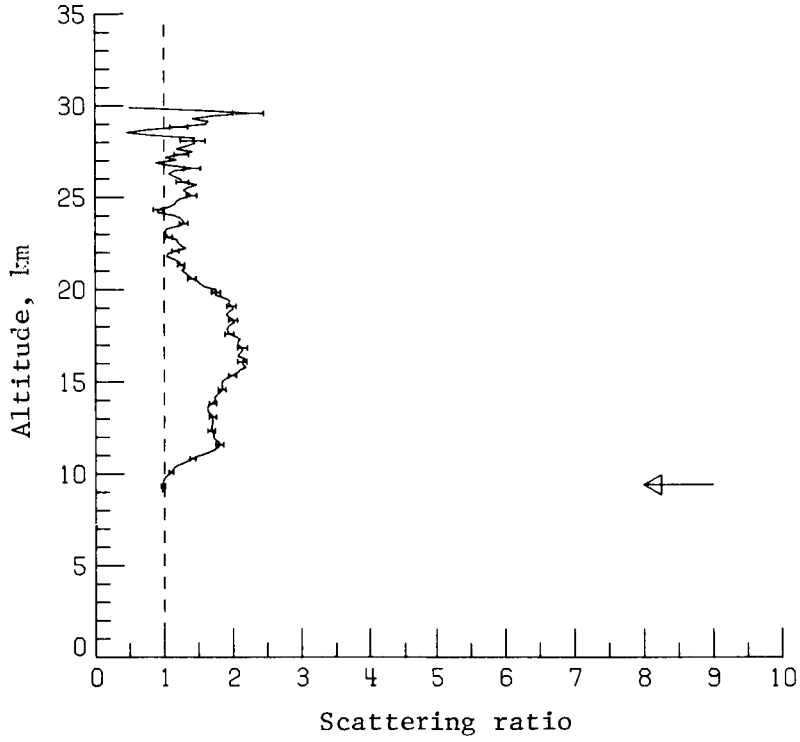

Figure 2. Lidar scattering-ratio profile taken on January 19, 1984, at GMT 2031–2052 between 41.3°N, 71.9°W and 42.8°N, 71.4°W.

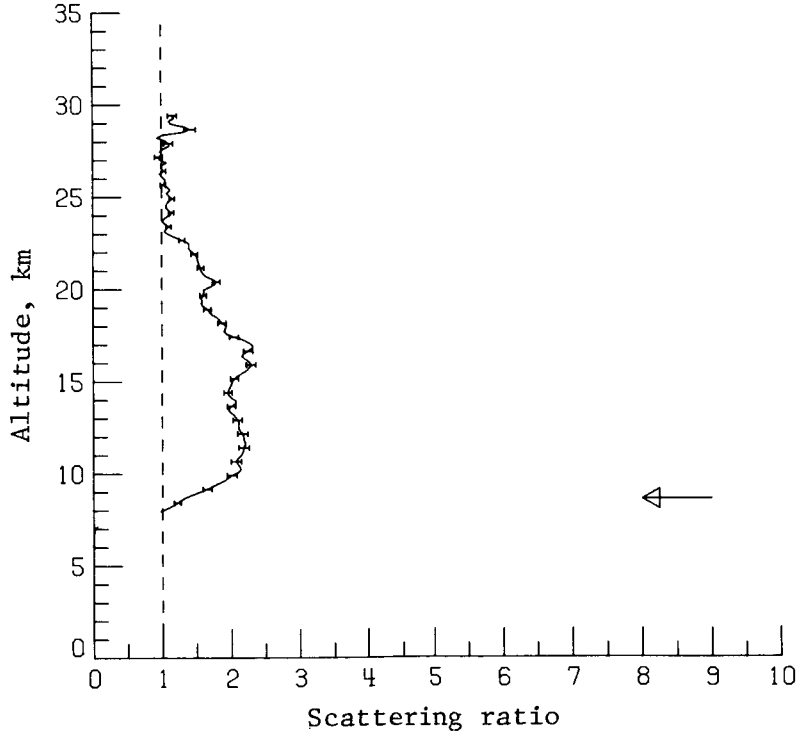

Figure 3. Lidar scattering-ratio profile taken on January 19, 1984, at GMT 2201–2218 between 48.6°N, 67.1°W and 50.2°N, 66.3°W.

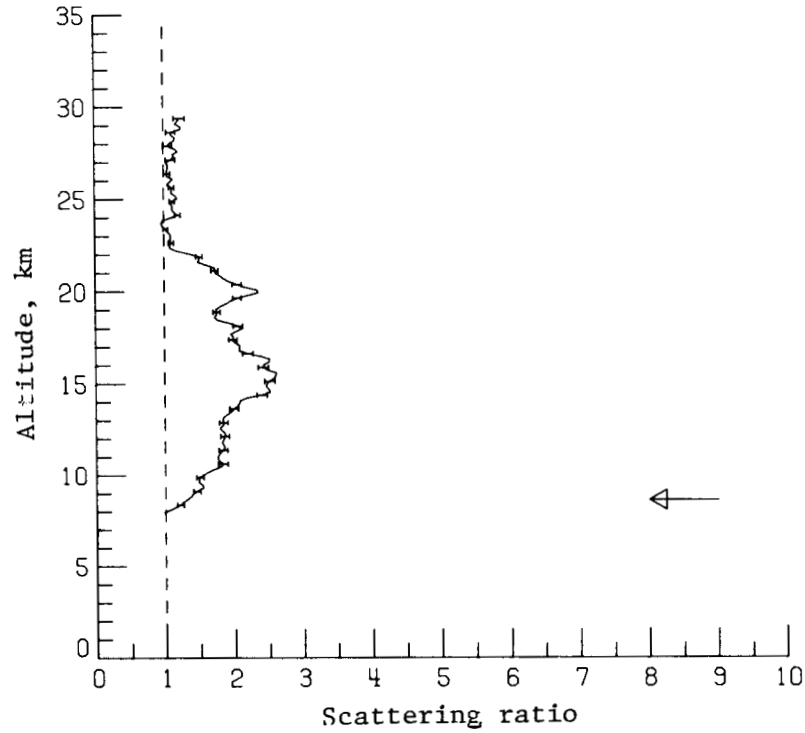

Figure 4. Lidar scattering-ratio profile taken on January 19, 1984, at GMT 2235–2249 between 51.5°N, 64.3°W and 52.5°N, 62.5°W.

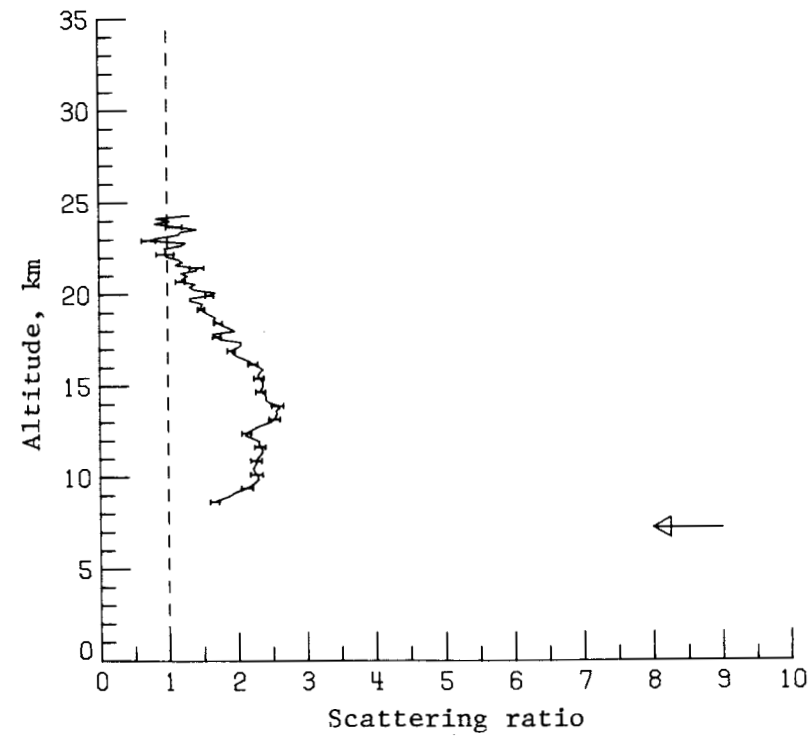

Figure 5. Lidar scattering-ratio profile taken on January 20, 1984, at GMT 1514–1527 between 56.4°N, 59.6°W and 57.6°N, 58.9°W.

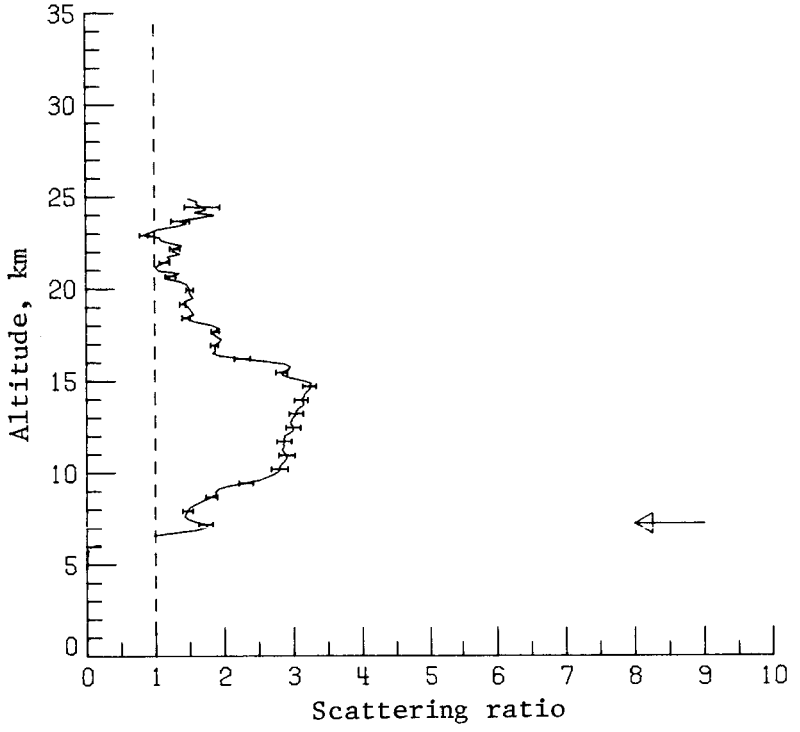

Figure 6. Lidar scattering-ratio profile taken on January 20, 1984, at GMT 1536–1549 between 58.3°N, 58.5°W and 59.3°N, 57.9°W.

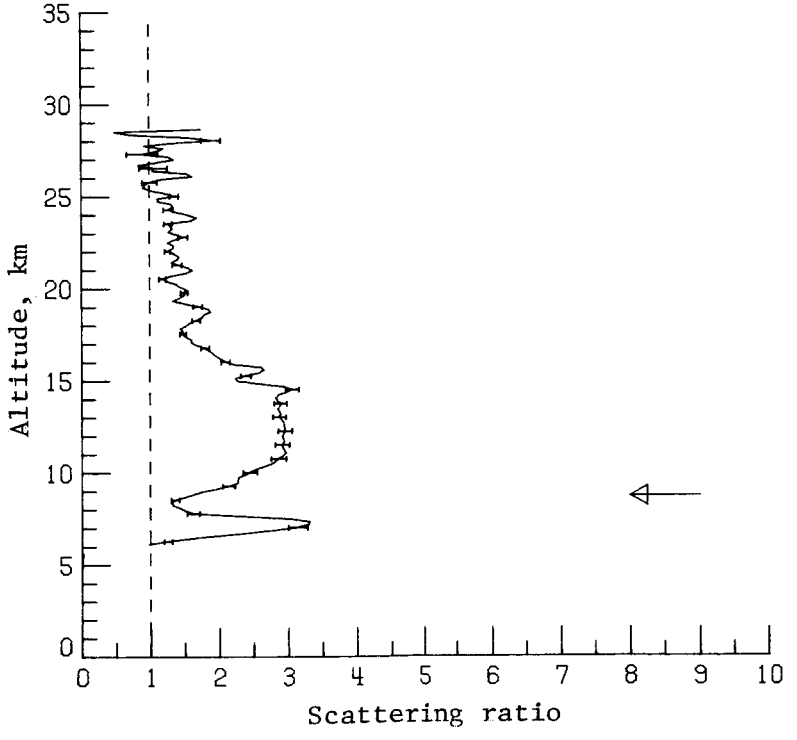

Figure 7. Lidar scattering-ratio profile taken on January 20, 1984, at GMT 1642–1702 between 63.4°N, 54.6°W and 65.0°N, 53.3°W.

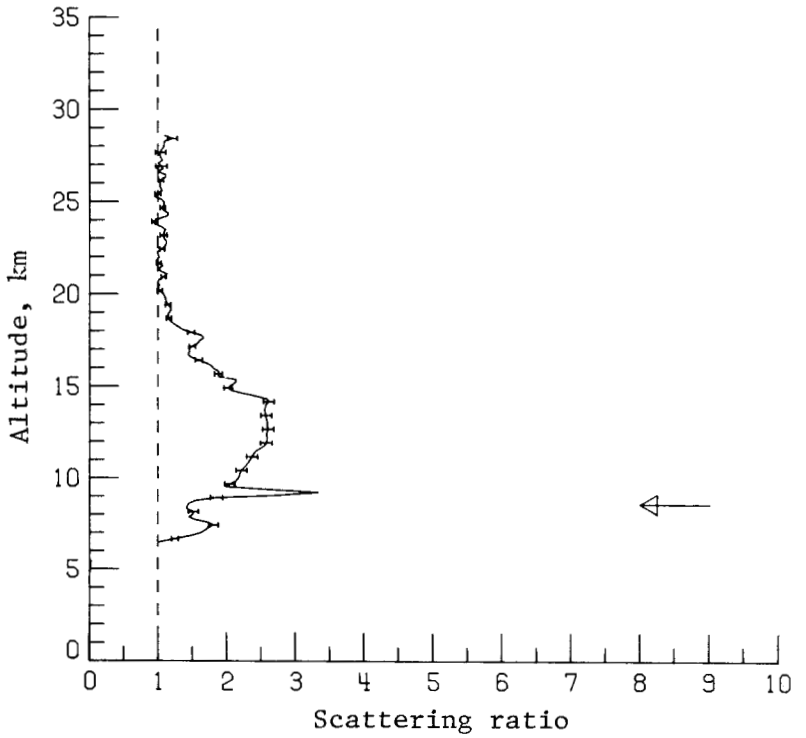

Figure 8. Lidar scattering-ratio profile taken on January 21, 1984, at GMT 1127–1144 between 67.0°N, 52.5°W and 67.5°N, 55.4°W.

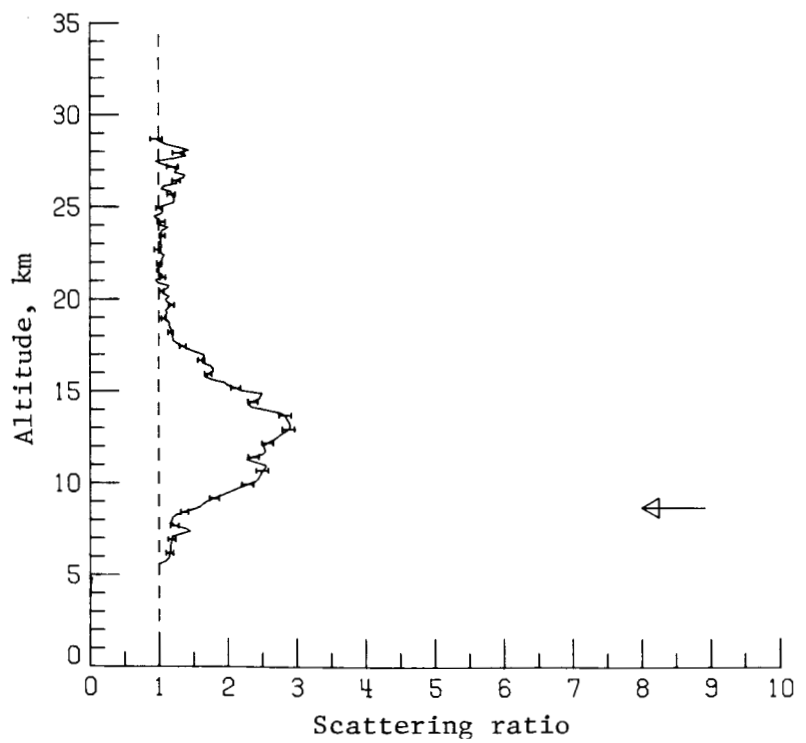

Figure 9. Lidar scattering-ratio profile taken on January 23, 1984, at GMT 1255–1313 between 67.8°N, 61.1°W and 68.0°N, 64.5°W.

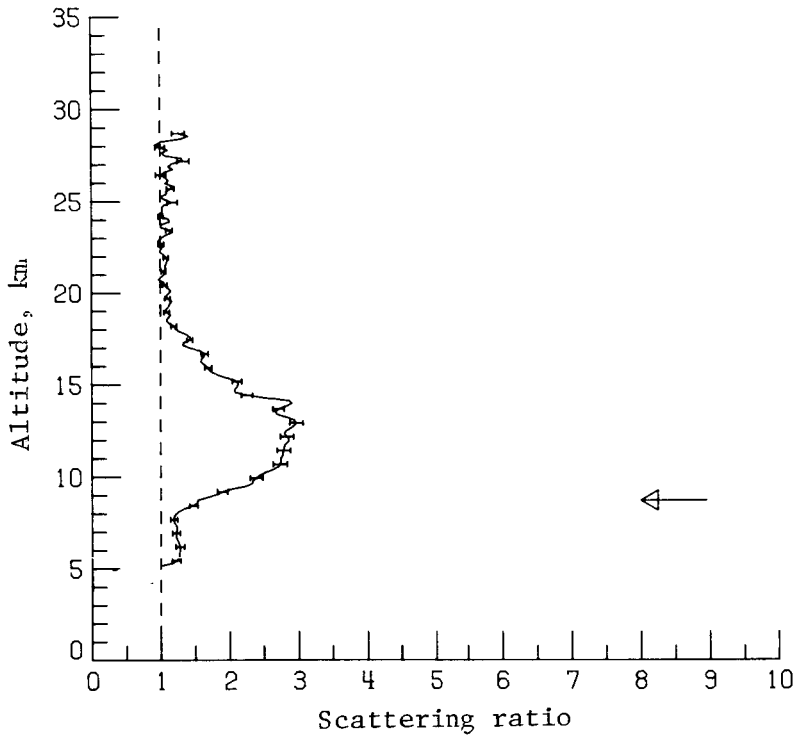

Figure 10. Lidar scattering-ratio profile taken on January 23, 1984, at GMT 1456–1506 between 69.7°N, 66.7°W and 70.4°N, 67.5°W.

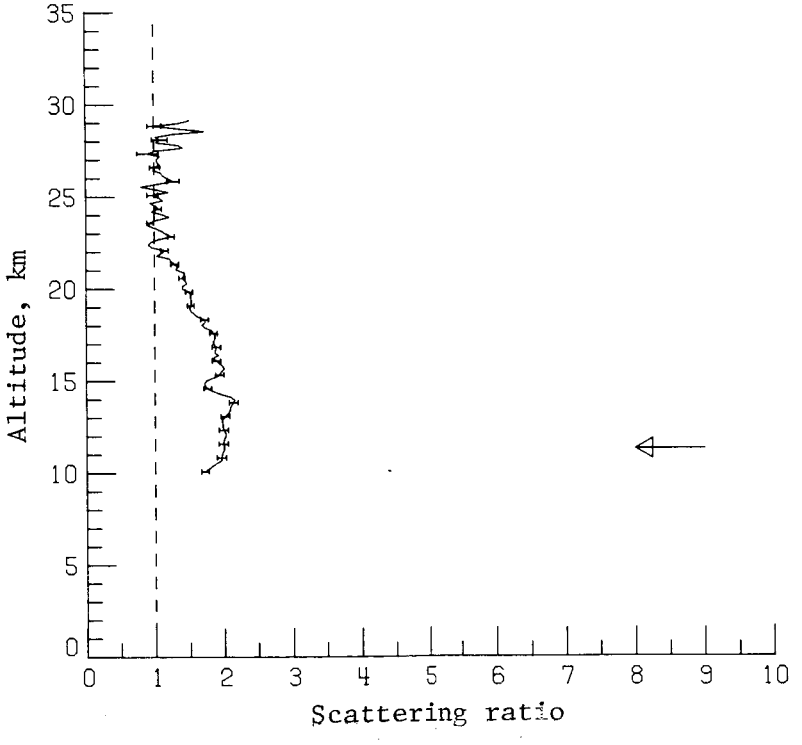

Figure 11. Lidar scattering-ratio profile taken on January 28, 1984, at GMT 1737–1751 between 55.7°N, 59.6°W and 54.9°N, 60.2°W.

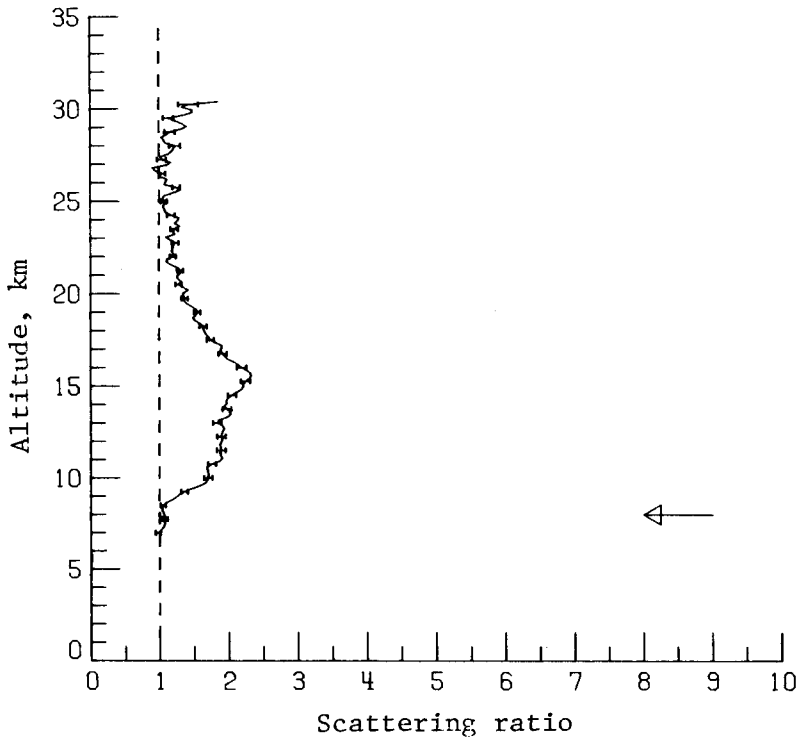

Figure 12. Lidar scattering-ratio profile taken on January 28, 1984, at GMT 2108–2120 between 50.8°N, 65.3°W and 50.2°N, 66.3°W.

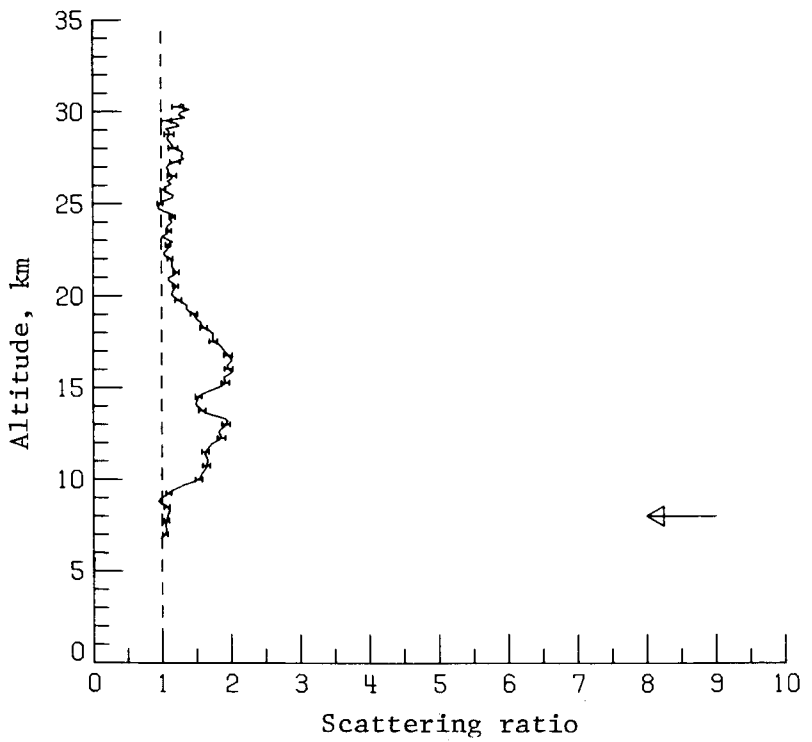

Figure 13. Lidar scattering-ratio profile taken on January 28, 1984, at GMT 2201–2217 between 47.2°N, 67.9°W and 46.1°N, 68.7°W.

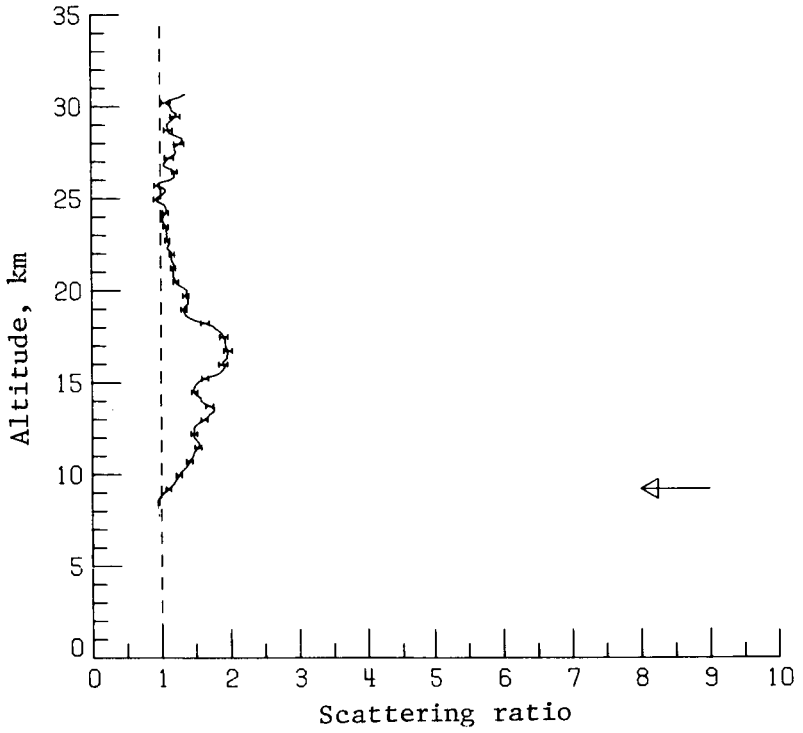

Figure 14. Lidar scattering-ratio profile taken on January 28, 1984, at GMT 2242–2254 between 44.3°N, 69.9°W and 43.5°N, 70.6°W.

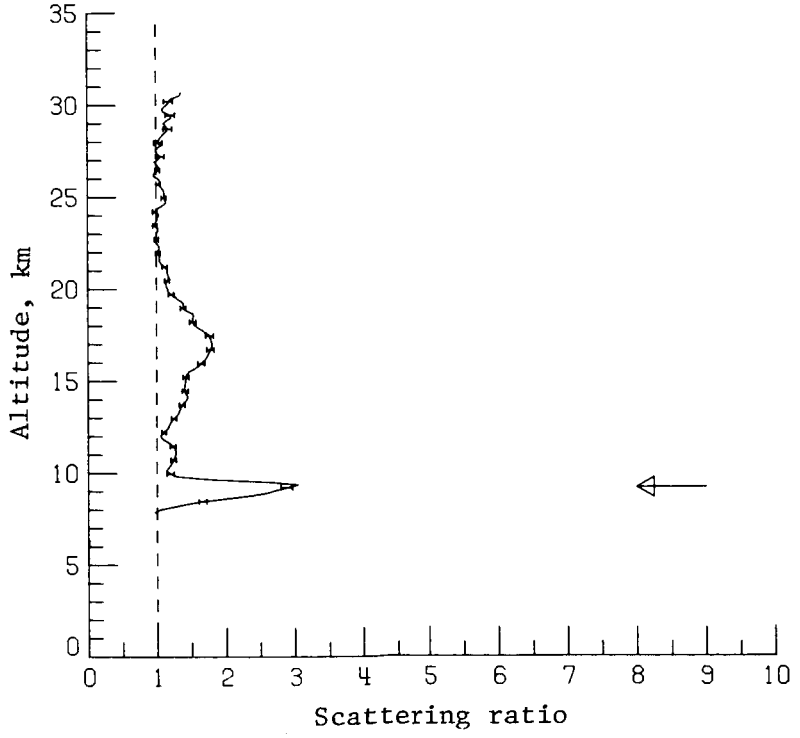

Figure 15. Lidar scattering-ratio profile taken on January 28, 1984, at GMT 2324–2349 between 41.4°N, 72.1°W and 39.8°N, 73.8°W.

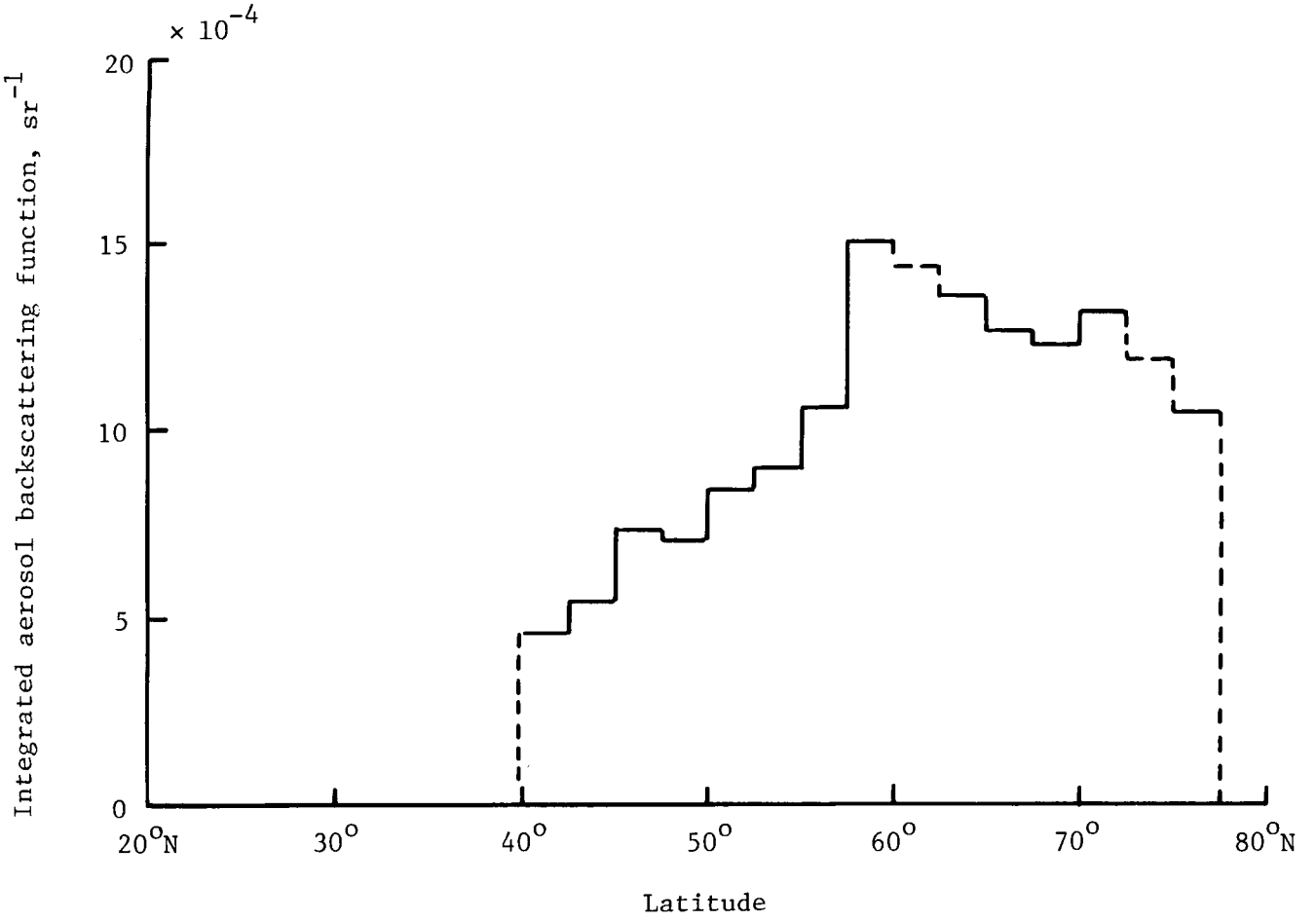

Figure 16. Integrated aerosol backscattering function from the tropopause through the stratospheric layer averaged into 2.5° latitude bins.

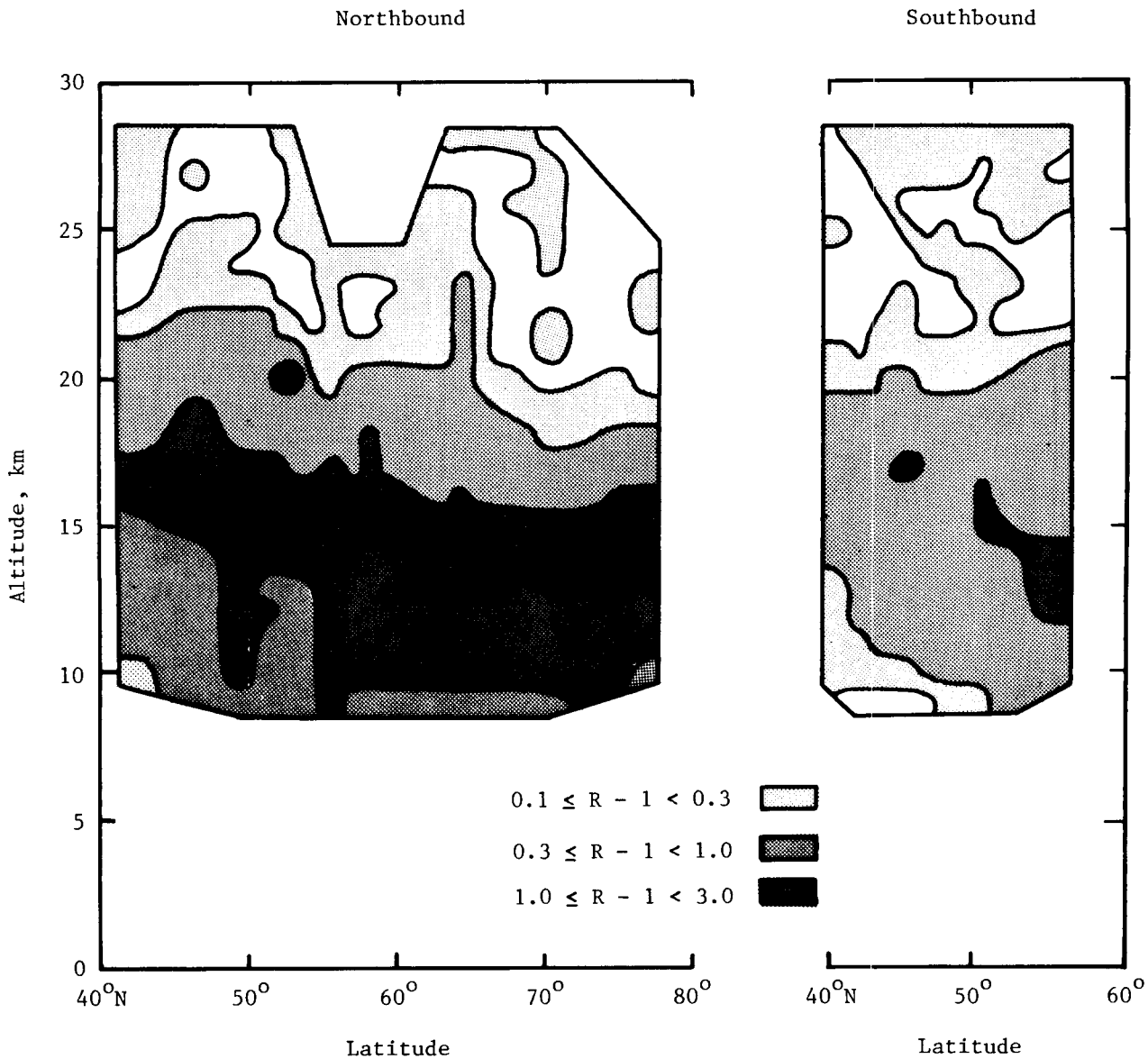

Figure 17. Contours of backscatter mixing ratio for data collected during southbound and northbound flight legs.

Appendix

Flight Log and Numerical Values of Scattering Ratios and Scattering Functions for Flight Mission

Table A1. Flight Log During Lidar Operation

Date	GMT[a]	Location	Altitude, ft
January 19	2031–2249	41.3°N, 71.9°W–52.5°N, 62.5°W	21 000
	2252–2257	52.6°N, 62.3°W–52.7°N, 61.7°W	13 000
	2300–2305	52.8°N, 61.3°W–53.0°N, 60.9°W	7 000
	2308–2314	53.1°N, 60.6°W–53.3°N, 60.3°W	3 000
January 20	1458–1603	54.8°N, 60.2°W–60.4°N, 57.2°W	17 000
	1625–1702	62.0°N, 55.9°W–65.0°N, 53.3°W	17 000
	1707–1714	65.3°N, 52.9°W–65.8°N, 52.4°W	13 000
	1724–1730	66.4°N, 51.6°W–66.6°N, 51.3°W	7 000
January 21	1127–1221	67.0°N, 52.5°W–69.8°N, 58.3°W	16 000
	1231–1312	69.8°N, 58.3°W–67.5°N, 55.4°W	16 000
	1318–1353	67.5°N, 55.4°W–69.8°N, 58.3°W	16 000
	1425–1434	67.9°N, 55.9°W–67.5°N, 55.3°W	16 000
January 23	1214–1250	67.2°N, 53.0°W–67.7°N, 60.1°W	16 000
	1255–1347	67.8°N, 61.1°W–70.4°N, 67.5°W	14 000
	1354–1425	70.4°N, 67.5°W–68.1°N, 65.1°W	14 000
	1430–1506	68.0°N, 64.8°W–70.4°N, 67.5°W	14 000
	1552–1607	74.5°N, 68.6°W–75.7°N, 68.5°W	29 000
	1617–1622	76.3°N, 68.3°W–76.2°N, 68.2°W	13 000
	1626–1630	76.2°N, 68.9°W–76.3°N, 69.6°W	7 000
January 28	1737–1751	55.7°N, 59.6°W–54.9°N, 60.2°W	24 000
	2026–2106	53.5°N, 60.1°W–50.9°N, 65.1°W	19 000
	2108–2217	50.8°N, 65.3°W–46.1°N, 68.7°W	16 000
	2223–2349	45.7°N, 69.0°W–39.8°N, 73.8°W	18 000

[a]Greenwich mean time.

Table A2. Lidar Data Taken on January 19, 1984, at GMT 2031–2052 Between 41.3°N, 71.9°W and 42.8°N, 71.4°W

Altitude, km	Scattering ratio	Scattering function, $(km\text{-}sr)^{-1}$	Altitude, km	Scattering ratio	Scattering function, $(km\text{-}sr)^{-1}$
9.768	1.008	.1350E-05	15.618	2.103	.8086E-04
9.918	1.049	.8359E-05	15.768	2.191	.8533E-04
10.068	1.099	.1647E-04	15.918	2.144	.8012E-04
10.218	1.127	.2075E-04	16.068	2.133	.7753E-04
10.368	1.162	.2576E-04	16.218	2.177	.7869E-04
10.518	1.249	.3875E-04	16.368	2.067	.6969E-04
10.668	1.342	.5203E-04	16.518	2.102	.7031E-04
10.818	1.414	.6163E-04	16.668	2.135	.7076E-04
10.968	1.516	.7505E-04	16.818	2.138	.6928E-04
11.118	1.630	.8951E-04	16.968	2.073	.6384E-04
11.268	1.720	.9991E-04	17.118	2.065	.6193E-04
11.418	1.774	.1050E-03	17.268	2.105	.6278E-04
11.568	1.799	.1061E-03	17.418	2.043	.5785E-04
11.718	1.781	.1015E-03	17.568	1.940	.5094E-04
11.868	1.726	.9234E-04	17.718	1.921	.4878E-04
12.018	1.714	.8882E-04	17.868	1.906	.4686E-04
12.168	1.710	.8654E-04	18.018	1.937	.4738E-04
12.318	1.683	.8138E-04	18.168	2.013	.4999E-04
12.468	1.684	.7983E-04	18.318	1.998	.4806E-04
12.618	1.692	.7902E-04	18.468	1.941	.4426E-04
12.768	1.698	.7807E-04	18.618	1.895	.4109E-04
12.918	1.693	.7581E-04	18.768	1.934	.4187E-04
13.068	1.699	.7483E-04	18.918	2.003	.4388E-04
13.218	1.677	.7091E-04	19.068	1.974	.4161E-04
13.368	1.636	.6522E-04	19.218	1.931	.3880E-04
13.518	1.628	.6291E-04	19.368	1.948	.3855E-04
13.668	1.637	.6246E-04	19.518	1.862	.3423E-04
13.818	1.701	.6717E-04	19.668	1.739	.2867E-04
13.968	1.734	.6883E-04	19.818	1.748	.2829E-04
14.118	1.727	.6660E-04	19.968	1.749	.2765E-04
14.268	1.760	.6808E-04	20.118	1.595	.2146E-04
14.418	1.809	.7094E-04	20.268	1.532	.1871E-04
14.568	1.832	.7132E-04	20.418	1.491	.1688E-04
14.718	1.839	.7034E-04	20.568	1.404	.1354E-04
14.868	1.830	.6799E-04	20.718	1.360	.1178E-04
15.018	1.836	.6704E-04	20.868	1.314	.1005E-04
15.168	1.898	.7037E-04	21.018	1.256	.7986E-05
15.318	1.988	.7569E-04	21.168	1.307	.9344E-05
15.468	2.058	.7934E-04	21.318	1.247	.7348E-05

Table A2. Concluded

Altitude, km	Scattering ratio	Scattering function, $(km\text{-}sr)^{-1}$	Altitude, km	Scattering ratio	Scattering function, $(km\text{-}sr)^{-1}$
21.468	1.217	.6286E-05	27.318	1.254	.2832E-05
21.618	1.144	.4074E-05	27.468	1.417	.4546E-05
21.768	1.037	.1019E-05	27.618	1.179	.1905E-05
21.918	1.048	.1290E-05	27.768	1.318	.3304E-05
22.068	1.163	.4287E-05	27.918	1.452	.4578E-05
22.218	1.321	.8245E-05	28.068	1.417	.4126E-05
22.368	1.249	.6239E-05	28.218	1.451	.4354E-05
22.518	1.201	.4929E-05	28.368	.828	-.1623E-05
22.668	1.188	.4500E-05	28.518	.458	-.4983E-05
22.818	1.062	.1456E-05	28.668	.766	-.2097E-05
22.968	1.030	.6737E-06	28.818	1.217	.1898E-05
23.118	1.020	.4382E-06	28.968	1.604	.5168E-05
23.268	1.025	.5355E-06	29.118	1.647	.5403E-05
23.418	1.213	.4510E-05	29.268	1.412	.3356E-05
23.568	1.287	.5929E-05	29.418	1.706	.5616E-05
23.718	1.274	.5516E-05	29.568	2.222	.9495E-05
23.868	1.238	.4680E-05	29.718	1.532	.4032E-05
24.018	1.118	.2254E-05	29.868	.507	-.3652E-05
24.168	.902	-.1828E-05			
24.318	.913	-.1583E-05			
24.468	1.080	.1427E-05			
24.618	1.157	.2727E-05			
24.768	1.181	.3066E-05			
24.918	1.246	.4050E-05			
25.068	1.400	.6436E-05			
25.218	1.346	.5433E-05			
25.368	1.279	.4275E-05			
25.518	1.349	.5206E-05			
25.668	1.482	.7015E-05			
25.818	1.266	.3777E-05			
25.968	1.244	.3387E-05			
26.118	1.148	.2006E-05			
26.268	1.069	.9088E-06			
26.418	1.143	.1839E-05			
26.568	1.409	.5149E-05			
26.718	1.088	.1086E-05			
26.868	.876	-.1485E-05			
27.018	1.181	.2120E-05			
27.168	1.012	.1414E-06			

Table A3. Lidar Data Taken on January 19, 1984, at GMT 2201–2218 Between 48.6°N, 67.1°W and 50.2°N, 66.3°W

Altitude, km	Scattering ratio	Scattering function, $(km\text{-}sr)^{-1}$	Altitude, km	Scattering ratio	Scattering function, $(km\text{-}sr)^{-1}$
8.116	1.077	.1687E-04	13.966	2.070	.9720E-04
8.266	1.154	.3331E-04	14.116	2.005	.8921E-04
8.416	1.221	.4679E-04	14.266	1.964	.8370E-04
8.566	1.279	.5779E-04	14.416	1.953	.8087E-04
8.716	1.351	.7096E-04	14.566	1.964	.7992E-04
8.866	1.452	.8926E-04	14.716	1.986	.7995E-04
9.016	1.557	.1075E-03	14.866	2.005	.7967E-04
9.166	1.653	.1232E-03	15.016	2.020	.7898E-04
9.316	1.730	.1346E-03	15.166	2.052	.7968E-04
9.466	1.811	.1460E-03	15.316	2.106	.8190E-04
9.616	1.898	.1581E-03	15.466	2.170	.8463E-04
9.766	1.949	.1633E-03	15.616	2.234	.8719E-04
9.916	2.013	.1701E-03	15.766	2.270	.8770E-04
10.066	2.102	.1807E-03	15.916	2.295	.8738E-04
10.216	2.142	.1829E-03	16.066	2.275	.8399E-04
10.366	2.132	.1771E-03	16.216	2.218	.7837E-04
10.516	2.101	.1683E-03	16.366	2.160	.7293E-04
10.666	2.076	.1606E-03	16.516	2.190	.7309E-04
10.816	2.096	.1598E-03	16.666	2.254	.7525E-04
10.966	2.143	.1627E-03	16.816	2.311	.7686E-04
11.116	2.166	.1621E-03	16.966	2.319	.7553E-04
11.266	2.181	.1606E-03	17.116	2.265	.7076E-04
11.416	2.190	.1582E-03	17.266	2.178	.6436E-04
11.566	2.206	.1570E-03	17.416	2.045	.5576E-04
11.716	2.205	.1534E-03	17.566	1.942	.4914E-04
11.866	2.186	.1476E-03	17.716	1.895	.4560E-04
12.016	2.186	.1444E-03	17.866	1.915	.4553E-04
12.166	2.170	.1393E-03	18.016	1.932	.4527E-04
12.316	2.134	.1320E-03	18.166	1.870	.4124E-04
12.466	2.110	.1264E-03	18.316	1.838	.3879E-04
12.616	2.112	.1238E-03	18.466	1.800	.3617E-04
12.766	2.117	.1216E-03	18.616	1.729	.3220E-04
12.916	2.095	.1167E-03	18.766	1.694	.2995E-04
13.066	2.069	.1114E-03	18.916	1.663	.2793E-04
13.216	2.034	.1052E-03	19.066	1.605	.2488E-04
13.366	1.976	.9706E-04	19.216	1.576	.2314E-04
13.516	1.961	.9342E-04	19.366	1.589	.2310E-04
13.666	2.004	.9546E-04	19.516	1.576	.2208E-04
13.816	2.071	.9950E-04	19.666	1.603	.2255E-04

Table A3. Concluded

Altitude, km	Scattering ratio	Scattering function, $(km\text{-}sr)^{-1}$	Altitude, km	Scattering ratio	Scattering function, $(km\text{-}sr)^{-1}$
19.816	1.614	.2240E-04	25.666	1.021	.2804E-06
19.966	1.611	.2172E-04	25.816	1.055	.7114E-06
20.116	1.692	.2400E-04	25.966	1.052	.6486E-06
20.266	1.761	.2574E-04	26.116	1.005	.6670E-07
20.416	1.790	.2605E-04	26.266	.971	-.3456E-06
20.566	1.724	.2328E-04	26.416	1.033	.3778E-06
20.716	1.636	.1996E-04	26.566	.997	-.3906E-07
20.866	1.601	.1839E-04	26.716	.994	-.6098E-07
21.016	1.573	.1711E-04	26.866	1.075	.8081E-06
21.166	1.568	.1653E-04	27.016	.980	-.2064E-06
21.316	1.549	.1559E-04	27.166	.958	-.4241E-06
21.466	1.535	.1481E-04	27.316	1.015	.1481E-06
21.616	1.522	.1408E-04	27.466	.977	-.2248E-06
21.766	1.519	.1366E-04	27.616	1.031	.2934E-06
21.916	1.480	.1232E-04	27.766	1.117	.1072E-05
22.066	1.439	.1098E-04	27.916	1.103	.9214E-06
22.216	1.395	.9643E-05	28.066	1.048	.4175E-06
22.366	1.403	.9587E-05	28.216	.936	-.5453E-06
22.516	1.396	.9197E-05	28.366	1.020	.1617E-06
22.666	1.297	.6734E-05	28.516	1.314	.2538E-05
22.816	1.203	.4475E-05	28.666	1.421	.3311E-05
22.966	1.113	.2413E-05	28.816	1.335	.2568E-05
23.116	1.040	.8334E-06	28.966	1.144	.1073E-05
23.266	1.061	.1235E-05	29.116	1.107	.7783E-06
23.416	1.101	.2006E-05	29.266	1.184	.1306E-05
23.566	1.041	.7913E-06	29.416	1.163	.1126E-05
23.716	1.003	.4984E-07			
23.866	1.045	.8168E-06			
24.016	1.120	.2121E-05			
24.166	1.143	.2463E-05			
24.316	1.095	.1604E-05			
24.466	1.058	.9448E-06			
24.616	1.070	.1108E-05			
24.766	1.100	.1553E-05			
24.916	1.153	.2304E-05			
25.066	1.113	.1661E-05			
25.216	1.070	.1003E-05			
25.366	1.128	.1779E-05			
25.516	1.094	.1270E-05			

Table A4. Lidar Data Taken on January 19, 1984, at GMT 2235–2249 Between 51.5°N, 64.3°W and 52.5°N, 62.5°W

Altitude, km	Scattering ratio	Scattering function, $(km\text{-}sr)^{-1}$	Altitude, km	Scattering ratio	Scattering function, $(km\text{-}sr)^{-1}$
8.087	1.055	.1224E-04	13.937	2.077	.9827E-04
8.237	1.141	.3054E-04	14.087	2.089	.9715E-04
8.387	1.212	.4508E-04	14.237	2.195	.1042E-03
8.537	1.255	.5292E-04	14.387	2.405	.1197E-03
8.687	1.311	.6318E-04	14.537	2.528	.1273E-03
8.837	1.366	.7273E-04	14.687	2.505	.1226E-03
8.987	1.398	.7714E-04	14.837	2.467	.1168E-03
9.137	1.453	.8577E-04	14.987	2.473	.1146E-03
9.287	1.540	.1000E-03	15.137	2.519	.1155E-03
9.437	1.542	.9813E-04	15.287	2.579	.1174E-03
9.587	1.489	.8639E-04	15.437	2.605	.1166E-03
9.737	1.478	.8260E-04	15.587	2.615	.1146E-03
9.887	1.499	.8424E-04	15.737	2.487	.1032E-03
10.037	1.553	.9118E-04	15.887	2.424	.9649E-04
10.187	1.625	.1006E-03	16.037	2.433	.9487E-04
10.337	1.714	.1122E-03	16.187	2.511	.9770E-04
10.487	1.812	.1246E-03	16.337	2.517	.9580E-04
10.637	1.838	.1257E-03	16.487	2.386	.8553E-04
10.787	1.785	.1150E-03	16.637	2.200	.7235E-04
10.937	1.758	.1085E-03	16.787	2.078	.6347E-04
11.087	1.773	.1079E-03	16.937	2.077	.6193E-04
11.237	1.797	.1088E-03	17.087	2.084	.6089E-04
11.387	1.842	.1124E-03	17.237	2.014	.5565E-04
11.537	1.864	.1129E-03	17.387	1.991	.5311E-04
11.687	1.844	.1079E-03	17.537	1.998	.5226E-04
11.837	1.827	.1034E-03	17.687	1.959	.4906E-04
11.987	1.849	.1038E-03	17.837	2.033	.5161E-04
12.137	1.866	.1036E-03	17.987	2.117	.5450E-04
12.287	1.872	.1020E-03	18.137	2.063	.5065E-04
12.437	1.826	.9451E-04	18.287	1.930	.4327E-04
12.587	1.794	.8880E-04	18.437	1.781	.3549E-04
12.737	1.843	.9220E-04	18.587	1.725	.3218E-04
12.887	1.850	.9093E-04	18.737	1.754	.3267E-04
13.037	1.837	.8753E-04	18.887	1.759	.3211E-04
13.187	1.849	.8677E-04	19.037	1.750	.3097E-04
13.337	1.910	.9090E-04	19.187	1.810	.3268E-04
13.487	1.965	.9429E-04	19.337	1.900	.3544E-04
13.637	1.999	.9542E-04	19.487	1.959	.3691E-04
13.787	2.047	.9770E-04	19.637	2.052	.3951E-04

Table A4. Concluded

Altitude, km	Scattering ratio	Scattering function, $(km\text{-}sr)^{-1}$	Altitude, km	Scattering ratio	Scattering function, $(km\text{-}sr)^{-1}$
19.787	2.206	.4419E-04	25.637	1.113	.1496E-05
19.937	2.364	.4874E-04	25.787	1.045	.5678E-06
20.087	2.330	.4635E-04	25.937	1.090	.1139E-05
20.237	2.158	.3937E-04	26.087	1.130	.1597E-05
20.387	2.051	.3482E-04	26.237	1.048	.5744E-06
20.537	1.935	.3023E-04	26.387	1.049	.5741E-06
20.687	1.865	.2725E-04	26.537	1.048	.5414E-06
20.837	1.814	.2504E-04	26.687	1.059	.6511E-06
20.987	1.743	.2227E-04	26.837	1.062	.6699E-06
21.137	1.733	.2144E-04	26.987	1.036	.3739E-06
21.287	1.732	.2086E-04	27.137	1.099	.1009E-05
21.437	1.599	.1667E-04	27.287	1.152	.1520E-05
21.587	1.481	.1304E-04	27.437	1.127	.1239E-05
21.737	1.505	.1334E-04	27.587	1.204	.1934E-05
21.887	1.505	.1303E-04	27.737	1.163	.1503E-05
22.037	1.366	.9195E-05	27.887	1.060	.5366E-06
22.187	1.188	.4612E-05	28.037	1.091	.8006E-06
22.337	1.088	.2117E-05	28.187	1.148	.1266E-05
22.487	1.080	.1871E-05	28.337	1.164	.1363E-05
22.637	1.102	.2310E-05	28.487	1.107	.8704E-06
22.787	1.085	.1893E-05	28.637	1.107	.8465E-06
22.937	1.096	.2060E-05	28.787	1.240	.1849E-05
23.087	1.093	.1958E-05	28.937	1.241	.1808E-05
23.237	1.049	.1011E-05	29.087	1.164	.1197E-05
23.387	1.025	.4873E-06	29.237	1.201	.1431E-05
23.537	.982	-.3528E-06	29.387	1.227	.1575E-05
23.687	.964	-.6733E-06			
23.837	.980	-.3665E-06			
23.987	1.093	.1660E-05			
24.137	1.196	.3407E-05			
24.287	1.151	.2542E-05			
24.437	1.112	.1846E-05			
24.587	1.123	.1972E-05			
24.737	1.105	.1627E-05			
24.887	1.118	.1793E-05			
25.037	1.191	.2811E-05			
25.187	1.165	.2368E-05			
25.337	1.103	.1435E-05			
25.487	1.114	.1554E-05			

Table A5. Lidar Data Taken on January 20, 1984, at GMT 1514–1527 Between 56.4°N, 59.6°W and 57.6°N, 58.9°W

Altitude, km	Scattering ratio	Scattering function, $(km\text{-}sr)^{-1}$	Altitude, km	Scattering ratio	Scattering function, $(km\text{-}sr)^{-1}$
8.671	1.665	.1325E-03	14.521	2.398	.1116E-03
8.821	1.767	.1488E-03	14.671	2.336	.1043E-03
8.971	1.872	.1648E-03	14.821	2.350	.1029E-03
9.121	1.934	.1719E-03	14.971	2.365	.1018E-03
9.271	2.019	.1826E-03	15.121	2.371	.9982E-04
9.421	2.133	.1979E-03	15.271	2.354	.9635E-04
9.571	2.209	.2062E-03	15.421	2.309	.9103E-04
9.721	2.256	.2092E-03	15.571	2.300	.8834E-04
9.871	2.297	.2110E-03	15.721	2.325	.8801E-04
10.021	2.296	.2060E-03	15.871	2.372	.8910E-04
10.171	2.270	.1970E-03	16.021	2.314	.8338E-04
10.321	2.240	.1879E-03	16.171	2.224	.7594E-04
10.471	2.219	.1805E-03	16.321	2.169	.7089E-04
10.621	2.244	.1798E-03	16.471	2.080	.6399E-04
10.771	2.265	.1787E-03	16.621	1.989	.5728E-04
10.921	2.265	.1745E-03	16.771	1.931	.5270E-04
11.071	2.296	.1749E-03	16.921	1.914	.5058E-04
11.221	2.334	.1761E-03	17.071	2.000	.5408E-04
11.371	2.355	.1749E-03	17.221	2.054	.5567E-04
11.521	2.359	.1715E-03	17.371	2.059	.5469E-04
11.671	2.321	.1630E-03	17.521	1.760	.3836E-04
11.821	2.312	.1583E-03	17.671	1.703	.3464E-04
11.971	2.314	.1550E-03	17.821	1.639	.3074E-04
12.121	2.218	.1405E-03	17.971	1.962	.4519E-04
12.271	2.110	.1253E-03	18.121	1.891	.4087E-04
12.421	2.126	.1242E-03	18.271	1.807	.3613E-04
12.571	2.203	.1298E-03	18.421	1.723	.3162E-04
12.721	2.270	.1340E-03	18.571	1.657	.2804E-04
12.871	2.377	.1419E-03	18.721	1.683	.2849E-04
13.021	2.483	.1494E-03	18.871	1.599	.2437E-04
13.171	2.535	.1511E-03	19.021	1.529	.2103E-04
13.321	2.554	.1494E-03	19.171	1.477	.1850E-04
13.471	2.569	.1475E-03	19.321	1.473	.1794E-04
13.621	2.565	.1437E-03	19.471	1.496	.1834E-04
13.771	2.608	.1443E-03	19.621	1.322	.1162E-04
13.921	2.583	.1387E-03	19.771	1.314	.1105E-04
14.071	2.462	.1252E-03	19.921	1.601	.2066E-04
14.221	2.411	.1180E-03	20.071	1.681	.2286E-04
14.371	2.416	.1156E-03	20.221	1.381	.1247E-04

Table A5. Concluded

Altitude, km	Scattering ratio	Scattering function, $(km\text{-}sr)^{-1}$	Altitude, km	Scattering ratio	Scattering function, $(km\text{-}sr)^{-1}$
20.371	1.313	.9995E-05			
20.521	1.392	.1222E-04			
20.671	1.180	.5493E-05			
20.821	1.219	.6499E-05			
20.971	1.280	.8131E-05			
21.121	1.193	.5469E-05			
21.271	1.410	.1134E-04			
21.421	1.418	.1126E-04			
21.571	1.115	.3018E-05			
21.721	1.215	.5517E-05			
21.871	1.157	.3937E-05			
22.021	1.000	.1117E-07			
22.171	.964	-.8644E-06			
22.321	.979	-.4845E-06			
22.471	.955	-.1031E-05			
22.621	1.185	.4089E-05			
22.771	1.259	.5575E-05			
22.921	.722	-.5822E-05			
23.071	.880	-.2454E-05			
23.221	1.155	.3068E-05			
23.371	1.190	.3657E-05			
23.521	1.418	.7849E-05			
23.671	1.095	.1736E-05			
23.821	.818	-.3228E-05			
23.971	1.030	.5109E-06			
24.121	.834	-.2787E-05			
24.271	1.302	.4937E-05			

Table A6. Lidar Data Taken on January 20, 1984, at GMT 1536–1549 Between 58.3°N, 58.5°W and 59.3°N, 57.9°W

Altitude, km	Scattering ratio	Scattering function, $(km\text{-}sr)^{-1}$	Altitude, km	Scattering ratio	Scattering function, $(km\text{-}sr)^{-1}$
6.721	1.245	.6539E-04	12.571	2.968	.2123E-03
6.871	1.580	.1517E-03	12.721	2.960	.2068E-03
7.021	1.758	.1939E-03	12.871	2.976	.2037E-03
7.171	1.727	.1919E-03	13.021	3.007	.2022E-03
7.321	1.572	.1402E-03	13.171	3.038	.2006E-03
7.471	1.464	.1113E-03	13.321	3.034	.1956E-03
7.621	1.425	.9983E-04	13.471	3.070	.1945E-03
7.771	1.444	.1019E-03	13.621	3.143	.1967E-03
7.921	1.469	.1054E-03	13.771	3.143	.1922E-03
8.071	1.491	.1079E-03	13.921	3.112	.1851E-03
8.221	1.551	.1187E-03	14.071	3.154	.1844E-03
8.371	1.638	.1340E-03	14.221	3.162	.1809E-03
8.521	1.716	.1465E-03	14.371	3.198	.1797E-03
8.671	1.814	.1622E-03	14.521	3.245	.1794E-03
8.821	1.879	.1706E-03	14.671	3.237	.1746E-03
8.971	1.874	.1653E-03	14.821	3.259	.1723E-03
9.121	1.925	.1702E-03	14.971	3.135	.1591E-03
9.271	2.074	.1926E-03	15.121	2.951	.1421E-03
9.421	2.312	.2292E-03	15.271	2.846	.1314E-03
9.571	2.513	.2580E-03	15.421	2.831	.1273E-03
9.721	2.613	.2687E-03	15.571	2.932	.1313E-03
9.871	2.713	.2788E-03	15.721	2.954	.1298E-03
10.021	2.777	.2824E-03	15.871	2.879	.1220E-03
10.171	2.800	.2794E-03	16.021	2.582	.1004E-03
10.321	2.800	.2729E-03	16.171	2.265	.7848E-04
10.471	2.835	.2717E-03	16.321	1.939	.5694E-04
10.621	2.878	.2715E-03	16.471	1.841	.4980E-04
10.771	2.897	.2680E-03	16.621	1.877	.5078E-04
10.921	2.902	.2625E-03	16.771	1.865	.4897E-04
11.071	2.859	.2508E-03	16.921	1.861	.4763E-04
11.221	2.835	.2422E-03	17.071	1.926	.5005E-04
11.371	2.862	.2403E-03	17.221	1.961	.5077E-04
11.521	2.852	.2337E-03	17.371	1.899	.4642E-04
11.671	2.865	.2301E-03	17.521	1.838	.4226E-04
11.821	2.866	.2252E-03	17.671	1.872	.4296E-04
11.971	2.868	.2205E-03	17.821	1.924	.4446E-04
12.121	2.943	.2242E-03	17.971	1.834	.3918E-04
12.271	2.993	.2248E-03	18.121	1.666	.3053E-04
12.421	2.994	.2200E-03	18.271	1.527	.2362E-04

Table A6. Concluded

Altitude, km	Scattering ratio	Scattering function, $(km\text{-}sr)^{-1}$	Altitude, km	Scattering ratio	Scattering function, $(km\text{-}sr)^{-1}$
18.421	1.452	.1977E-04	24.271	1.745	.1219E-04
18.571	1.560	.2391E-04	24.421	1.691	.1100E-04
18.721	1.539	.2248E-04	24.571	1.602	.9323E-05
18.871	1.510	.2077E-04	24.721	1.615	.9266E-05
19.021	1.479	.1903E-04	24.871	1.490	.7183E-05
19.171	1.404	.1569E-04			
19.321	1.442	.1676E-04			
19.471	1.547	.2024E-04			
19.621	1.523	.1890E-04			
19.771	1.500	.1763E-04			
19.921	1.507	.1744E-04			
20.071	1.488	.1639E-04			
20.221	1.462	.1513E-04			
20.371	1.374	.1196E-04			
20.521	1.175	.5447E-05			
20.671	1.229	.6984E-05			
20.821	1.345	.1025E-04			
20.971	1.053	.1537E-05			
21.121	1.014	.4059E-06			
21.271	1.054	.1492E-05			
21.421	1.140	.3783E-05			
21.571	1.224	.5883E-05			
21.721	1.186	.4790E-05			
21.871	1.364	.9114E-05			
22.021	1.256	.6263E-05			
22.171	1.296	.7075E-05			
22.321	1.392	.9144E-05			
22.471	1.219	.4991E-05			
22.621	1.096	.2128E-05			
22.771	1.072	.1560E-05			
22.921	.845	-.3246E-05			
23.071	.945	-.1117E-05			
23.221	1.041	.8167E-06			
23.371	1.308	.5946E-05			
23.521	1.459	.8619E-05			
23.671	1.376	.6870E-05			
23.821	1.616	.1094E-04			
23.971	1.862	.1489E-04			
24.121	1.591	.9941E-05			

Table A7. Lidar Data Taken on January 20, 1984, at GMT 1642–1702 Between 63.4°N, 54.6°W and 65.0°N, 53.3°W

Altitude, km	Scattering ratio	Scattering function, $(km\text{-}sr)^{-1}$	Altitude, km	Scattering ratio	Scattering function, $(km\text{-}sr)^{-1}$
6.284	1.259	.7270E-04	12.134	2.934	.2239E-03
6.434	1.577	.1590E-03	12.284	2.959	.2213E-03
6.584	2.011	.2732E-03	12.434	2.953	.2157E-03
6.734	2.443	.3825E-03	12.584	2.943	.2097E-03
6.884	2.819	.4725E-03	12.734	2.933	.2041E-03
7.034	3.143	.5456E-03	12.884	2.901	.1963E-03
7.184	3.302	.5743E-03	13.034	2.877	.1895E-03
7.334	3.318	.5670E-03	13.184	2.892	.1867E-03
7.484	3.056	.4929E-03	13.334	2.873	.1808E-03
7.634	2.310	.3079E-03	13.484	2.852	.1748E-03
7.784	1.623	.1435E-03	13.634	2.884	.1739E-03
7.934	1.503	.1136E-03	13.784	2.891	.1706E-03
8.084	1.424	.9392E-04	13.934	2.840	.1623E-03
8.234	1.327	.7088E-04	14.084	2.828	.1577E-03
8.384	1.308	.6517E-04	14.234	2.862	.1571E-03
8.534	1.365	.7556E-04	14.384	2.982	.1635E-03
8.684	1.506	.1025E-03	14.534	3.066	.1667E-03
8.834	1.633	.1254E-03	14.684	2.925	.1518E-03
8.984	1.769	.1492E-03	14.834	2.577	.1216E-03
9.134	1.981	.1859E-03	14.984	2.273	.9603E-04
9.284	2.142	.2117E-03	15.134	2.246	.9176E-04
9.434	2.270	.2295E-03	15.284	2.393	.1001E-03
9.584	2.274	.2246E-03	15.434	2.592	.1117E-03
9.734	2.281	.2201E-03	15.584	2.656	.1135E-03
9.884	2.385	.2322E-03	15.734	2.615	.1080E-03
10.034	2.451	.2372E-03	15.884	2.223	.7983E-04
10.184	2.528	.2436E-03	16.034	2.099	.7009E-04
10.334	2.647	.2562E-03	16.184	2.031	.6418E-04
10.484	2.762	.2672E-03	16.334	1.961	.5836E-04
10.634	2.817	.2688E-03	16.484	1.914	.5422E-04
10.784	2.864	.2690E-03	16.634	1.864	.5000E-04
10.934	2.928	.2715E-03	16.784	1.802	.4535E-04
11.084	2.964	.2700E-03	16.934	1.678	.3740E-04
11.234	2.943	.2606E-03	17.084	1.605	.3260E-04
11.384	2.920	.2512E-03	17.234	1.601	.3160E-04
11.534	2.919	.2450E-03	17.384	1.517	.2655E-04
11.684	2.941	.2418E-03	17.534	1.482	.2415E-04
11.834	2.931	.2347E-03	17.684	1.473	.2310E-04
11.984	2.915	.2272E-03	17.834	1.449	.2140E-04

Table A7. Concluded

Altitude, km	Scattering ratio	Scattering function, $(km\text{-}sr)^{-1}$	Altitude, km	Scattering ratio	Scattering function, $(km\text{-}sr)^{-1}$
17.984	1.531	.2472E-04	23.834	1.686	.1132E-04
18.134	1.574	.2605E-04	23.984	1.572	.9151E-05
18.284	1.675	.2991E-04	24.134	1.397	.6155E-05
18.434	1.762	.3293E-04	24.284	1.272	.4097E-05
18.584	1.789	.3327E-04	24.434	1.338	.4967E-05
18.734	1.884	.3638E-04	24.584	1.318	.4554E-05
18.884	1.857	.3444E-04	24.734	1.123	.1723E-05
19.034	1.698	.2734E-04	24.884	1.112	.1525E-05
19.184	1.501	.1917E-04	25.034	1.361	.4810E-05
19.334	1.337	.1255E-04	25.184	1.212	.2759E-05
19.484	1.430	.1563E-04	25.334	1.000	-.1590E-08
19.634	1.497	.1763E-04	25.484	.906	-.1163E-05
19.784	1.501	.1734E-04	25.634	.922	-.9476E-06
19.934	1.536	.1810E-04	25.784	1.002	.2099E-07
20.084	1.440	.1449E-04	25.934	1.171	.1965E-05
20.234	1.387	.1241E-04	26.084	1.612	.6887E-05
20.384	1.253	.7908E-05	26.234	1.540	.5931E-05
20.534	1.186	.5677E-05	26.384	1.044	.4758E-06
20.684	1.311	.9262E-05	26.534	1.057	.5993E-06
20.834	1.534	.1551E-04	26.684	.833	-.1710E-05
20.984	1.620	.1757E-04	26.834	1.098	.9737E-06
21.134	1.544	.1502E-04	26.984	1.356	.3460E-05
21.284	1.399	.1075E-04	27.134	1.286	.2718E-05
21.434	1.319	.8378E-05	27.284	.892	-.1000E-05
21.584	1.402	.1031E-04	27.434	1.104	.9415E-06
21.734	1.427	.1066E-04	27.584	1.203	.1796E-05
21.884	1.356	.8681E-05	27.734	.929	-.6144E-06
22.034	1.260	.6188E-05	27.884	1.319	.2683E-05
22.184	1.340	.7839E-05	28.034	1.900	.7386E-05
22.334	1.347	.7773E-05	28.184	1.574	.4601E-05
22.484	1.261	.5662E-05	28.334	.736	-.2068E-05
22.634	1.345	.7276E-05	28.484	.488	-.3910E-05
22.784	1.487	.9955E-05	28.634	1.746	.5557E-05
22.934	1.383	.7589E-05			
23.084	1.269	.5161E-05			
23.234	1.323	.6021E-05			
23.384	1.301	.5444E-05			
23.534	1.269	.4719E-05			
23.684	1.602	.1023E-04			

Table A8. Lidar Data Taken on January 21, 1984, at GMT 1127–1144 Between 67.0°N, 52.5°W and 67.5°N, 55.4°W

Altitude, km	Scattering ratio	Scattering function, $(km\text{-}sr)^{-1}$	Altitude, km	Scattering ratio	Scattering function, $(km\text{-}sr)^{-1}$
6.527	1.063	.1714E-04	12.377	2.571	.1725E-03
6.677	1.245	.6511E-04	12.527	2.584	.1699E-03
6.827	1.442	.1150E-03	12.677	2.598	.1674E-03
6.977	1.602	.1534E-03	12.827	2.584	.1622E-03
7.127	1.681	.1702E-03	12.977	2.587	.1587E-03
7.277	1.729	.1788E-03	13.127	2.582	.1546E-03
7.427	1.804	.1934E-03	13.277	2.569	.1497E-03
7.577	1.727	.1713E-03	13.427	2.570	.1464E-03
7.727	1.544	.1257E-03	13.577	2.554	.1415E-03
7.877	1.449	.1018E-03	13.727	2.548	.1377E-03
8.027	1.506	.1124E-03	13.877	2.560	.1356E-03
8.177	1.515	.1120E-03	14.027	2.569	.1332E-03
8.327	1.417	.8860E-04	14.177	2.609	.1334E-03
8.477	1.421	.8746E-04	14.327	2.582	.1282E-03
8.627	1.448	.9082E-04	14.477	2.417	.1122E-03
8.777	1.544	.1079E-03	14.627	2.227	.9489E-04
8.927	1.850	.1646E-03	14.777	2.074	.8111E-04
9.077	2.760	.3332E-03	14.927	2.017	.7504E-04
9.227	3.328	.4302E-03	15.077	2.067	.7684E-04
9.377	2.657	.2984E-03	15.227	2.130	.7936E-04
9.527	1.991	.1739E-03	15.377	2.129	.7743E-04
9.677	2.044	.1787E-03	15.527	1.882	.5900E-04
9.827	2.123	.1873E-03	15.677	1.877	.5723E-04
9.977	2.164	.1892E-03	15.827	1.879	.5599E-04
10.127	2.180	.1870E-03	15.977	1.804	.4995E-04
10.277	2.189	.1837E-03	16.127	1.777	.4712E-04
10.427	2.212	.1825E-03	16.277	1.697	.4127E-04
10.577	2.248	.1832E-03	16.427	1.590	.3410E-04
10.727	2.286	.1843E-03	16.577	1.484	.2728E-04
10.877	2.314	.1838E-03	16.727	1.436	.2397E-04
11.027	2.341	.1830E-03	16.877	1.456	.2445E-04
11.177	2.365	.1818E-03	17.027	1.449	.2351E-04
11.327	2.386	.1803E-03	17.177	1.496	.2535E-04
11.477	2.419	.1800E-03	17.327	1.577	.2878E-04
11.627	2.483	.1837E-03	17.477	1.603	.2933E-04
11.777	2.549	.1872E-03	17.627	1.665	.3154E-04
11.927	2.572	.1855E-03	17.777	1.631	.2924E-04
12.077	2.583	.1823E-03	17.927	1.480	.2168E-04
12.227	2.587	.1784E-03	18.077	1.364	.1605E-04

Table A8. Concluded

Altitude, km	Scattering ratio	Scattering function, $(km\text{-}sr)^{-1}$	Altitude, km	Scattering ratio	Scattering function, $(km\text{-}sr)^{-1}$
18.227	1.296	.1275E-04	24.077	1.015	.2389E-06
18.377	1.231	.9695E-05	24.227	1.133	.2029E-05
18.527	1.183	.7502E-05	24.377	1.153	.2266E-05
18.677	1.157	.6277E-05	24.527	1.081	.1171E-05
18.827	1.141	.5494E-05	24.677	1.067	.9472E-06
18.977	1.157	.5958E-05	24.827	1.089	.1228E-05
19.127	1.185	.6879E-05	24.977	1.090	.1214E-05
19.277	1.184	.6681E-05	25.127	1.052	.6857E-06
19.427	1.145	.5127E-05	25.277	.947	-.6789E-06
19.577	1.120	.4137E-05	25.427	.996	-.4836E-07
19.727	1.113	.3791E-05	25.577	1.064	.7761E-06
19.877	1.098	.3212E-05	25.727	1.039	.4622E-06
20.027	1.075	.2418E-05	25.877	1.027	.3175E-06
20.177	1.025	.7913E-06	26.027	1.033	.3797E-06
20.327	1.000	-.1290E-07	26.177	1.043	.4736E-06
20.477	1.020	.6002E-06	26.327	1.110	.1190E-05
20.627	.998	-.5192E-07	26.477	1.112	.1178E-05
20.777	1.013	.3581E-06	26.627	.995	-.5640E-07
20.927	1.060	.2224E-05	26.777	1.074	.7419E-06
21.077	1.134	.3624E-05	26.927	1.050	.4921E-06
21.227	1.043	.1140E-05	27.077	1.005	.4798E-07
21.377	1.011	.2855E-06	27.227	1.064	.5955E-06
21.527	1.071	.1783E-05	27.377	1.048	.4350E-06
21.677	1.014	.3313E-06	27.527	1.025	.2183E-06
21.827	.975	-.6068E-06	27.677	1.038	.3290E-06
21.977	1.019	.4382E-06	27.827	1.054	.4617E-06
22.127	1.005	.1163E-06	27.977	1.087	.7227E-06
22.277	.988	-.2660E-06	28.127	1.089	.7195E-06
22.427	1.060	.1280E-05	28.277	1.097	.7673E-06
22.577	1.097	.2015E-05	28.427	1.211	.1622E-05
22.727	1.124	.2507E-05	28.577	1.101	.7627E-06
22.877	1.122	.2405E-05			
23.027	1.084	.1613E-05			
23.177	1.081	.1514E-05			
23.327	1.086	.1548E-05			
23.477	1.111	.1944E-05			
23.627	1.057	.9775E-06			
23.777	.959	-.6791E-06			
23.927	.938	-.9928E-06			

Table A9. Lidar Data Taken on January 23, 1984, at GMT 1255–1313 Between 67.8°N, 61.1°W and 68.0°N, 64.5°W

Altitude, km	Scattering ratio	Scattering function, $(km\text{-}sr)^{-1}$	Altitude, km	Scattering ratio	Scattering function, $(km\text{-}sr)^{-1}$
5.587	1.002	.7108E-06	11.437	2.373	.1781E-03
5.737	1.093	.2780E-04	11.587	2.511	.1915E-03
5.887	1.139	.4071E-04	11.737	2.547	.1915E-03
6.037	1.151	.4337E-04	11.887	2.532	.1852E-03
6.187	1.155	.4372E-04	12.037	2.516	.1790E-03
6.337	1.167	.4612E-04	12.187	2.578	.1820E-03
6.487	1.167	.4543E-04	12.337	2.658	.1868E-03
6.637	1.170	.4520E-04	12.487	2.716	.1888E-03
6.787	1.180	.4706E-04	12.637	2.765	.1896E-03
6.937	1.187	.4792E-04	12.787	2.828	.1916E-03
7.087	1.188	.4732E-04	12.937	2.881	.1926E-03
7.237	1.315	.7776E-04	13.087	2.910	.1908E-03
7.387	1.458	.1108E-03	13.237	2.898	.1852E-03
7.537	1.387	.9194E-04	13.387	2.875	.1786E-03
7.687	1.226	.5260E-04	13.537	2.851	.1721E-03
7.837	1.173	.3964E-04	13.687	2.833	.1664E-03
7.987	1.187	.4202E-04	13.837	2.749	.1550E-03
8.137	1.200	.4392E-04	13.987	2.561	.1351E-03
8.287	1.253	.5459E-04	14.137	2.354	.1144E-03
8.437	1.370	.7808E-04	14.287	2.289	.1063E-03
8.587	1.504	.1039E-03	14.437	2.364	.1098E-03
8.737	1.599	.1209E-03	14.587	2.457	.1146E-03
8.887	1.642	.1267E-03	14.737	2.471	.1129E-03
9.037	1.703	.1357E-03	14.887	2.500	.1124E-03
9.187	1.804	.1520E-03	15.037	2.201	.8781E-04
9.337	1.905	.1670E-03	15.187	2.115	.7951E-04
9.487	1.993	.1785E-03	15.337	2.004	.6986E-04
9.637	2.089	.1907E-03	15.487	1.947	.6431E-04
9.787	2.182	.2016E-03	15.637	1.765	.5071E-04
9.937	2.288	.2139E-03	15.787	1.677	.4379E-04
10.087	2.396	.2259E-03	15.937	1.715	.4513E-04
10.237	2.443	.2275E-03	16.087	1.787	.4843E-04
10.387	2.463	.2246E-03	16.237	1.784	.4708E-04
10.537	2.485	.2221E-03	16.387	1.745	.4369E-04
10.687	2.502	.2191E-03	16.537	1.641	.3664E-04
10.837	2.546	.2203E-03	16.687	1.614	.3426E-04
10.987	2.548	.2155E-03	16.837	1.651	.3544E-04
11.137	2.408	.1914E-03	16.987	1.649	.3450E-04
11.287	2.276	.1695E-03	17.137	1.535	.2776E-04

Table A9. Concluded

Altitude, km	Scattering ratio	Scattering function, $(km\text{-}sr)^{-1}$	Altitude, km	Scattering ratio	Scattering function, $(km\text{-}sr)^{-1}$
17.287	1.423	.2145E-04	23.137	1.032	.6172E-06
17.437	1.347	.1721E-04	23.287	1.028	.5392E-06
17.587	1.269	.1302E-04	23.437	1.053	.9777E-06
17.737	1.210	.9931E-05	23.587	1.022	.3976E-06
17.887	1.202	.9303E-05	23.737	1.056	.9752E-06
18.037	1.202	.9104E-05	23.887	1.130	.2231E-05
18.187	1.170	.7491E-05	24.037	1.014	.2402E-06
18.337	1.181	.7770E-05	24.187	1.040	.6426E-06
18.487	1.160	.6708E-05	24.337	.985	-.2358E-06
18.637	1.152	.6248E-05	24.487	.935	-.1004E-05
18.787	1.142	.5700E-05	24.637	1.039	.5799E-06
18.937	1.074	.2914E-05	24.787	1.062	.9105E-06
19.087	1.094	.3582E-05	24.937	1.008	.1102E-06
19.237	1.121	.4516E-05	25.087	1.089	.1233E-05
19.387	1.102	.3702E-05	25.237	1.217	.2940E-05
19.537	1.139	.4930E-05	25.387	1.220	.2905E-05
19.687	1.185	.6397E-05	25.537	1.219	.2816E-05
19.837	1.125	.4213E-05	25.687	1.181	.2267E-05
19.987	1.097	.3205E-05	25.837	1.178	.2171E-05
20.137	1.150	.4826E-05	25.987	1.035	.4158E-06
20.287	1.071	.2243E-05	26.137	1.078	.9010E-06
20.437	1.042	.1291E-05	26.287	1.262	.2952E-05
20.587	1.126	.3753E-05	26.437	1.254	.2791E-05
20.737	1.145	.4239E-05	26.587	1.355	.3791E-05
20.887	.987	-.3821E-06	26.737	1.380	.3952E-05
21.037	.956	-.1216E-05	26.887	1.230	.2333E-05
21.187	1.059	.1608E-05	27.037	1.258	.2546E-05
21.337	1.044	.1172E-05	27.187	1.201	.1933E-05
21.487	.966	-.8648E-06	27.337	1.041	.3829E-06
21.637	.974	-.6627E-06	27.487	.959	-.3745E-06
21.787	1.045	.1100E-05	27.637	1.213	.1890E-05
21.937	1.009	.2051E-06	27.787	1.394	.3409E-05
22.087	1.043	.9943E-06	27.937	1.286	.2407E-05
22.237	1.053	.1198E-05	28.087	1.430	.3531E-05
22.387	1.081	.1784E-05	28.237	1.304	.2428E-05
22.537	1.018	.3894E-06	28.387	1.127	.9924E-06
22.687	.983	-.3622E-06	28.537	1.029	.2212E-06
22.837	1.047	.9692E-06	28.687	.966	-.2542E-06
22.987	1.026	.5144E-06			

Table A10. Lidar Data Taken on January 23, 1984, at GMT 1456–1506 Between 69.7°N, 66.7°W and 70.4°N, 67.5°W

Altitude, km	Scattering ratio	Scattering function, $(km\text{-}sr)^{-1}$	Altitude, km	Scattering ratio	Scattering function, $(km\text{-}sr)^{-1}$
5.287	1.167	.5254E-04	11.137	2.767	.2402E-03
5.437	1.223	.6887E-04	11.287	2.772	.2354E-03
5.587	1.264	.8013E-04	11.437	2.783	.2313E-03
5.737	1.269	.8011E-04	11.587	2.788	.2266E-03
5.887	1.270	.7907E-04	11.737	2.799	.2226E-03
6.037	1.277	.7955E-04	11.887	2.847	.2233E-03
6.187	1.276	.7778E-04	12.037	2.862	.2198E-03
6.337	1.267	.7370E-04	12.187	2.830	.2110E-03
6.487	1.248	.6730E-04	12.337	2.795	.2022E-03
6.637	1.230	.6117E-04	12.487	2.814	.1995E-03
6.787	1.221	.5781E-04	12.637	2.882	.2020E-03
6.937	1.221	.5668E-04	12.787	2.937	.2030E-03
7.087	1.228	.5741E-04	12.937	2.964	.2010E-03
7.237	1.239	.5899E-04	13.087	2.938	.1936E-03
7.387	1.217	.5254E-04	13.237	2.824	.1780E-03
7.537	1.189	.4482E-04	13.387	2.693	.1612E-03
7.687	1.186	.4337E-04	13.537	2.658	.1542E-03
7.837	1.190	.4350E-04	13.687	2.710	.1552E-03
7.987	1.218	.4896E-04	13.837	2.819	.1612E-03
8.137	1.270	.5935E-04	13.987	2.907	.1650E-03
8.287	1.349	.7531E-04	14.137	2.861	.1572E-03
8.437	1.472	.9961E-04	14.287	2.517	.1251E-03
8.587	1.526	.1085E-03	14.437	2.248	.1005E-03
8.737	1.534	.1078E-03	14.587	2.079	.8481E-04
8.887	1.666	.1314E-03	14.737	2.069	.8203E-04
9.037	1.809	.1562E-03	14.887	2.105	.8278E-04
9.187	1.890	.1682E-03	15.037	2.121	.8193E-04
9.337	2.028	.1897E-03	15.187	2.103	.7865E-04
9.487	2.227	.2205E-03	15.337	1.996	.6931E-04
9.637	2.324	.2319E-03	15.487	1.959	.5837E-04
9.787	2.335	.2276E-03	15.637	1.762	.5050E-04
9.937	2.386	.2302E-03	15.787	1.702	.4543E-04
10.087	2.440	.2331E-03	15.937	1.685	.4321E-04
10.237	2.517	.2391E-03	16.087	1.638	.3926E-04
10.387	2.624	.2494E-03	16.237	1.581	.3492E-04
10.537	2.702	.2546E-03	16.387	1.593	.3474E-04
10.687	2.730	.2525E-03	16.537	1.625	.3575E-04
10.837	2.743	.2484E-03	16.687	1.637	.3554E-04
10.987	2.736	.2417E-03	16.837	1.570	.3104E-04

Table A10. Concluded

Altitude, km	Scattering ratio	Scattering function, $(km\text{-}sr)^{-1}$	Altitude, km	Scattering ratio	Scattering function, $(km\text{-}sr)^{-1}$
16.987	1.436	.2316E-04	22.837	.960	-.8173E-06
17.137	1.325	.1636E-04	22.987	1.004	.7429E-07
17.287	1.332	.1685E-04	23.137	1.063	.1219E-05
17.437	1.422	.2092E-04	23.287	1.159	.3025E-05
17.587	1.431	.2085E-04	23.437	1.126	.2336E-05
17.737	1.366	.1729E-04	23.587	1.003	.5706E-07
17.887	1.273	.1261E-04	23.737	1.006	.1067E-06
18.037	1.212	.9583E-05	23.887	1.137	.2348E-05
18.187	1.193	.8505E-05	24.037	1.115	.1912E-05
18.337	1.124	.5348E-05	24.187	1.004	.7030E-07
18.487	1.085	.3591E-05	24.337	1.024	.3747E-06
18.637	1.111	.4573E-05	24.487	1.027	.4184E-06
18.787	1.145	.5831E-05	24.637	1.020	.2962E-06
18.937	1.088	.3461E-05	24.787	1.046	.6724E-06
19.087	1.078	.2989E-05	24.937	1.172	.2458E-05
19.237	1.117	.4376E-05	25.087	1.074	.1022E-05
19.387	1.131	.4783E-05	25.237	1.001	.1530E-07
19.537	1.165	.5860E-05	25.387	1.089	.1179E-05
19.687	1.100	.3461E-05	25.537	1.085	.1094E-05
19.837	1.080	.2705E-05	25.687	1.145	.1809E-05
19.987	1.128	.4218E-05	25.837	1.177	.2159E-05
20.137	1.148	.4752E-05	25.987	1.072	.8547E-06
20.287	1.093	.2920E-05	26.137	1.122	.1407E-05
20.437	1.065	.1983E-05	26.287	1.076	.8521E-06
20.587	1.046	.1380E-05	26.437	1.008	.8904E-07
20.737	.969	-.8894E-06	26.587	1.065	.6903E-06
20.887	1.013	.3599E-06	26.737	1.183	.1900E-05
21.037	1.066	.1822E-05	26.887	1.114	.1155E-05
21.187	1.045	.1208E-05	27.037	1.163	.1610E-05
21.337	1.079	.2079E-05	27.187	1.332	.3191E-05
21.487	1.068	.1760E-05	27.337	1.302	.2827E-05
21.637	1.085	.2132E-05	27.487	1.065	.5926E-06
21.787	1.104	.2543E-05	27.637	1.026	.2289E-06
21.937	1.079	.1886E-05	27.787	1.106	.9210E-06
22.087	1.055	.1281E-05	27.937	.995	-.4544E-07
22.237	.991	-.2104E-06	28.087	.942	-.4768E-06
22.387	1.003	.7607E-07	28.237	1.016	.1294E-06
22.537	1.036	.7807E-06	28.387	1.301	.2342E-05
22.687	1.016	.2003E-06	28.537	1.405	.3076E-05

Table A11. Lidar Data Taken on January 28, 1984, at GMT 1737–1751 Between 55.7°N, 59.6°W and 54.9°N, 60.2°W

Altitude, km	Scattering ratio	Scattering function, $(km\text{-}sr)^{-1}$	Altitude, km	Scattering ratio	Scattering function, $(km\text{-}sr)^{-1}$
10.090	1.724	.1206E-03	15.940	1.939	.6186E-04
10.240	1.781	.1277E-03	16.090	1.893	.5745E-04
10.390	1.831	.1333E-03	16.240	1.841	.5285E-04
10.540	1.897	.1410E-03	16.390	1.921	.5656E-04
10.690	1.962	.1483E-03	16.540	1.869	.5210E-04
10.840	1.964	.1458E-03	16.690	1.881	.5158E-04
10.990	1.965	.1431E-03	16.840	1.894	.5115E-04
11.140	1.983	.1429E-03	16.990	1.855	.4777E-04
11.290	2.001	.1418E-03	17.140	1.848	.4629E-04
11.440	1.998	.1376E-03	17.290	1.874	.4660E-04
11.590	1.992	.1332E-03	17.440	1.875	.4556E-04
11.740	1.992	.1298E-03	17.590	1.853	.4335E-04
11.890	2.005	.1281E-03	17.740	1.821	.4076E-04
12.040	2.027	.1274E-03	17.890	1.731	.3541E-04
12.190	2.018	.1231E-03	18.040	1.680	.3215E-04
12.340	1.995	.1171E-03	18.190	1.731	.3372E-04
12.490	1.980	.1124E-03	18.340	1.722	.3248E-04
12.640	1.983	.1097E-03	18.490	1.621	.2728E-04
12.790	1.971	.1056E-03	18.640	1.569	.2439E-04
12.940	1.977	.1035E-03	18.790	1.523	.2184E-04
13.090	2.018	.1053E-03	18.940	1.506	.2064E-04
13.240	2.057	.1068E-03	19.090	1.525	.2087E-04
13.390	2.084	.1069E-03	19.240	1.526	.2041E-04
13.540	2.089	.1049E-03	19.390	1.532	.2013E-04
13.690	2.107	.1041E-03	19.540	1.515	.1902E-04
13.840	2.140	.1047E-03	19.690	1.528	.1901E-04
13.990	2.153	.1034E-03	19.840	1.500	.1759E-04
14.140	2.091	.9554E-04	19.990	1.402	.1381E-04
14.290	1.955	.8169E-04	20.140	1.402	.1347E-04
14.440	1.840	.7015E-04	20.290	1.469	.1538E-04
14.590	1.766	.6243E-04	20.440	1.441	.1411E-04
14.740	1.722	.5750E-04	20.590	1.397	.1241E-04
14.890	1.712	.5538E-04	20.740	1.428	.1307E-04
15.040	1.751	.5701E-04	20.890	1.430	.1286E-04
15.190	1.865	.6415E-04	21.040	1.306	.8932E-05
15.340	1.942	.6821E-04	21.190	1.337	.9609E-05
15.490	1.957	.6764E-04	21.340	1.294	.8198E-05
15.640	2.002	.6918E-04	21.490	1.241	.6567E-05
15.790	1.989	.6670E-04	21.640	1.217	.5787E-05

Table A11. Concluded

Altitude, km	Scattering ratio	Scattering function, $(km\text{-}sr)^{-1}$	Altitude, km	Scattering ratio	Scattering function, $(km\text{-}sr)^{-1}$
21.790	1.033	.8677E-06	27.640	1.419	.4314E-05
21.940	1.097	.2470E-05	27.790	1.356	.3574E-05
22.090	1.147	.3645E-05	27.940	1.032	.3166E-06
22.240	.961	-.9524E-06	28.090	1.084	.8011E-06
22.390	.911	-.2104E-05	28.240	1.022	.2061E-06
22.540	.944	-.1288E-05	28.390	1.259	.2359E-05
22.690	1.060	.1354E-05	28.540	1.726	.6450E-05
22.840	1.242	.5362E-05	28.690	1.361	.3135E-05
22.990	1.165	.3554E-05	28.840	1.006	.4818E-07
23.140	1.105	.2211E-05	28.990	1.355	.2937E-05
23.290	1.009	.1862E-06	29.140	1.511	.4119E-05
23.440	.907	-.1864E-05			
23.590	.940	-.1173E-05			
23.740	1.038	.7383E-06			
23.890	1.213	.4003E-05			
24.040	1.111	.2030E-05			
24.190	.965	-.6302E-06			
24.340	1.056	.9732E-06			
24.490	1.028	.4739E-06			
24.640	.939	-.1011E-05			
24.790	1.122	.1989E-05			
24.940	1.064	.1024E-05			
25.090	.975	-.3939E-06			
25.240	1.201	.3041E-05			
25.390	1.021	.3171E-06			
25.540	.807	-.2792E-05			
25.690	1.044	.6254E-06			
25.840	1.277	.3812E-05			
25.990	1.196	.2637E-05			
26.140	1.124	.1623E-05			
26.290	1.095	.1213E-05			
26.440	.986	-.1785E-06			
26.590	1.013	.1527E-06			
26.740	1.072	.8612E-06			
26.890	1.041	.4788E-06			
27.040	1.033	.3797E-06			
27.190	1.079	.8701E-06			
27.340	.909	-.9792E-06			
27.490	1.015	.1563E-06			

Table A12. Lidar Data Taken on January 28, 1984, at GMT 2108–2120 Between 50.8°N, 65.3°W and 50.2°N, 66.3°W

Altitude, km	Scattering ratio	Scattering function, $(km\text{-}sr)^{-1}$	Altitude, km	Scattering ratio	Scattering function, $(km\text{-}sr)^{-1}$
7.008	.980	-.5051E-05	12.858	1.907	.9654E-04
7.158	1.022	.5393E-05	13.008	1.834	.8685E-04
7.308	1.058	.1393E-04	13.158	1.854	.8695E-04
7.458	1.077	.1828E-04	13.308	1.976	.9714E-04
7.608	1.075	.1747E-04	13.458	2.029	.1000E-03
7.758	1.078	.1776E-04	13.608	2.019	.9684E-04
7.908	1.077	.1720E-04	13.758	1.976	.9064E-04
8.058	1.059	.1298E-04	13.908	1.932	.8461E-04
8.208	1.040	.8667E-05	14.058	1.975	.8655E-04
8.358	1.039	.8136E-05	14.208	1.964	.8366E-04
8.508	1.054	.1109E-04	14.358	1.988	.8383E-04
8.658	1.105	.2129E-04	14.508	2.050	.8705E-04
8.808	1.183	.3624E-04	14.658	2.108	.8980E-04
8.958	1.243	.4691E-04	14.808	2.184	.9382E-04
9.108	1.289	.5455E-04	14.958	2.208	.9351E-04
9.258	1.360	.6631E-04	15.108	2.211	.9169E-04
9.408	1.460	.8281E-04	15.258	2.244	.9202E-04
9.558	1.576	.1013E-03	15.408	2.297	.9377E-04
9.708	1.657	.1129E-03	15.558	2.326	.9376E-04
9.858	1.690	.1159E-03	15.708	2.313	.9069E-04
10.008	1.704	.1154E-03	15.858	2.255	.8481E-04
10.158	1.706	.1132E-03	16.008	2.186	.7844E-04
10.308	1.705	.1104E-03	16.158	2.139	.7373E-04
10.458	1.691	.1057E-03	16.308	2.076	.6814E-04
10.608	1.690	.1030E-03	16.458	1.986	.6112E-04
10.758	1.759	.1108E-03	16.608	1.946	.5739E-04
10.908	1.867	.1237E-03	16.758	1.915	.5431E-04
11.058	1.907	.1263E-03	16.908	1.884	.5138E-04
11.208	1.885	.1205E-03	17.058	1.899	.5110E-04
11.358	1.877	.1167E-03	17.208	1.903	.5025E-04
11.508	1.893	.1162E-03	17.358	1.811	.4413E-04
11.658	1.884	.1125E-03	17.508	1.740	.3942E-04
11.808	1.874	.1088E-03	17.658	1.712	.3710E-04
11.958	1.893	.1087E-03	17.808	1.674	.3437E-04
12.108	1.912	.1085E-03	17.958	1.656	.3274E-04
12.258	1.895	.1041E-03	18.108	1.636	.3105E-04
12.408	1.896	.1020E-03	18.258	1.636	.3032E-04
12.558	1.918	.1022E-03	18.408	1.590	.2746E-04
12.708	1.938	.1021E-03	18.558	1.514	.2334E-04

Table A12. Concluded

Altitude, km	Scattering ratio	Scattering function, $(km\text{-}sr)^{-1}$	Altitude, km	Scattering ratio	Scattering function, $(km\text{-}sr)^{-1}$
18.708	1.490	.2172E-04	24.558	1.082	.1453E-05
18.858	1.530	.2296E-04	24.708	1.055	.9475E-06
19.008	1.552	.2336E-04	24.858	1.081	.1358E-05
19.158	1.534	.2202E-04	25.008	1.071	.1164E-05
19.308	1.475	.1915E-04	25.158	1.052	.8282E-06
19.458	1.405	.1593E-04	25.308	1.074	.1163E-05
19.608	1.360	.1385E-04	25.458	1.198	.3022E-05
19.758	1.371	.1393E-04	25.608	1.299	.4462E-05
19.908	1.346	.1269E-04	25.758	1.253	.3681E-05
20.058	1.353	.1263E-04	25.908	1.080	.1130E-05
20.208	1.423	.1476E-04	26.058	1.097	.1338E-05
20.358	1.341	.1162E-04	26.208	1.115	.1561E-05
20.508	1.281	.9362E-05	26.358	.995	-.6604E-07
20.658	1.321	.1047E-04	26.508	1.048	.6232E-06
20.808	1.267	.8509E-05	26.658	.943	-.7129E-06
20.958	1.255	.7940E-05	26.808	.902	-.1207E-05
21.108	1.309	.9408E-05	26.958	1.112	.1338E-05
21.258	1.305	.9077E-05	27.108	1.172	.2017E-05
21.408	1.269	.7821E-05	27.258	1.043	.4886E-06
21.558	1.176	.4983E-05	27.408	1.018	.1963E-06
21.708	1.112	.3099E-05	27.558	1.139	.1514E-05
21.858	1.112	.3047E-05	27.708	1.181	.1925E-05
22.008	1.200	.5292E-05	27.858	1.213	.2213E-05
22.158	1.205	.5301E-05	28.008	1.231	.2345E-05
22.308	1.182	.4600E-05	28.158	1.091	.9062E-06
22.458	1.198	.4889E-05	28.308	1.071	.6852E-06
22.608	1.198	.4777E-05	28.458	1.036	.3434E-06
22.758	1.236	.5571E-05	28.608	1.105	.9731E-06
22.908	1.166	.3838E-05	28.758	1.159	.1431E-05
23.058	1.096	.2159E-05	28.908	1.318	.2794E-05
23.208	1.230	.5081E-05	29.058	1.400	.3433E-05
23.358	1.197	.4249E-05	29.208	1.336	.2821E-05
23.508	1.220	.4624E-05	29.358	1.241	.1973E-05
23.658	1.300	.6168E-05	29.508	1.140	.1117E-05
23.808	1.224	.4485E-05	29.658	1.335	.2617E-05
23.958	1.265	.5176E-05	29.808	1.480	.3660E-05
24.108	1.288	.5503E-05	29.958	1.482	.3591E-05
24.258	1.175	.3256E-05	30.108	1.332	.2415E-05
24.408	1.094	.1712E-05	30.258	1.429	.3042E-05

Table A13. Lidar Data Taken on January 28, 1984, at GMT 2201–2217 Between 47.2°N, 67.9°W and 46.1°N, 68.7°W

Altitude, km	Scattering ratio	Scattering function, $(km\text{-}sr)^{-1}$	Altitude, km	Scattering ratio	Scattering function, $(km\text{-}sr)^{-1}$
6.858	1.002	.4222E-06	12.708	1.845	.9196E-04
7.008	1.043	.1086E-04	12.858	1.895	.9525E-04
7.158	1.064	.1556E-04	13.008	1.927	.9644E-04
7.308	1.059	.1428E-04	13.158	1.950	.9671E-04
7.458	1.056	.1312E-04	13.308	1.917	.9126E-04
7.608	1.056	.1298E-04	13.458	1.780	.7588E-04
7.758	1.066	.1489E-04	13.608	1.640	.6080E-04
7.908	1.076	.1687E-04	13.758	1.582	.5410E-04
8.058	1.082	.1784E-04	13.908	1.542	.4923E-04
8.208	1.106	.2280E-04	14.058	1.496	.4402E-04
8.358	1.111	.2347E-04	14.208	1.498	.4323E-04
8.508	1.072	.1479E-04	14.358	1.513	.4351E-04
8.658	.999	-.1213E-06	14.508	1.529	.4390E-04
8.808	.950	-.9844E-05	14.658	1.594	.4812E-04
8.958	.974	-.5086E-05	14.808	1.684	.5418E-04
9.108	1.041	.7763E-05	14.958	1.788	.6103E-04
9.258	1.096	.1776E-04	15.108	1.877	.6638E-04
9.408	1.153	.2745E-04	15.258	1.918	.6790E-04
9.558	1.231	.4067E-04	15.408	1.911	.6589E-04
9.708	1.322	.5537E-04	15.558	1.898	.6348E-04
9.858	1.437	.7342E-04	15.708	1.969	.6697E-04
10.008	1.531	.8706E-04	15.858	2.020	.6894E-04
10.158	1.560	.8971E-04	16.008	1.966	.6392E-04
10.308	1.576	.9016E-04	16.158	1.942	.6099E-04
10.458	1.605	.9255E-04	16.308	1.972	.6158E-04
10.608	1.632	.9444E-04	16.458	2.012	.6272E-04
10.758	1.643	.9391E-04	16.608	1.994	.6027E-04
10.908	1.655	.9343E-04	16.758	1.959	.5692E-04
11.058	1.662	.9218E-04	16.908	1.924	.5365E-04
11.208	1.646	.8795E-04	17.058	1.892	.5070E-04
11.358	1.621	.8268E-04	17.208	1.862	.4793E-04
11.508	1.626	.8151E-04	17.358	1.814	.4432E-04
11.658	1.661	.8418E-04	17.508	1.746	.3972E-04
11.808	1.689	.8574E-04	17.658	1.732	.3817E-04
11.958	1.724	.8813E-04	17.808	1.745	.3803E-04
12.108	1.798	.9497E-04	17.958	1.737	.3681E-04
12.258	1.859	.1000E-03	18.108	1.682	.3331E-04
12.408	1.847	.9638E-04	18.258	1.608	.2899E-04
12.558	1.820	.9126E-04	18.408	1.572	.2663E-04

Table A13. Concluded

Altitude, km	Scattering ratio	Scattering function, $(km\text{-}sr)^{-1}$	Altitude, km	Scattering ratio	Scattering function, $(km\text{-}sr)^{-1}$
18.558	1.564	.2565E-04	24.408	1.165	.2988E-05
18.708	1.510	.2262E-04	24.558	1.054	.9593E-06
18.858	1.484	.2098E-04	24.708	.962	-.6527E-06
19.008	1.465	.1965E-04	24.858	.952	-.8050E-06
19.158	1.388	.1600E-04	25.008	.981	-.3112E-06
19.308	1.354	.1427E-04	25.158	1.050	.8068E-06
19.458	1.369	.1452E-04	25.308	1.157	.2461E-05
19.608	1.303	.1162E-04	25.458	1.173	.2642E-05
19.758	1.239	.8960E-05	25.608	1.082	.1225E-05
19.908	1.193	.6709E-05	25.758	1.023	.3289E-06
20.058	1.146	.5225E-05	25.908	1.063	.8966E-06
20.208	1.159	.5561E-05	26.058	1.141	.1957E-05
20.358	1.183	.6245E-05	26.208	1.088	.1195E-05
20.508	1.201	.6712E-05	26.358	1.153	.2024E-05
20.658	1.167	.5449E-05	26.508	1.154	.1981E-05
20.808	1.104	.3317E-05	26.658	1.102	.1288E-05
20.958	1.098	.3047E-05	26.808	1.101	.1247E-05
21.108	1.180	.5481E-05	26.958	1.076	.9147E-06
21.258	1.212	.6292E-05	27.108	1.105	.1229E-05
21.408	1.178	.5174E-05	27.258	1.198	.2265E-05
21.558	1.152	.4319E-05	27.408	1.323	.3607E-05
21.708	1.145	.4029E-05	27.558	1.284	.3103E-05
21.858	1.154	.4182E-05	27.708	1.314	.3339E-05
22.008	1.125	.3319E-05	27.858	1.278	.2886E-05
22.158	1.050	.1303E-05	28.008	1.172	.1751E-05
22.308	1.032	.8166E-06	28.158	1.156	.1547E-05
22.458	1.076	.1889E-05	28.308	1.129	.1245E-05
22.608	1.100	.2411E-05	28.458	1.093	.8788E-06
22.758	1.095	.2248E-05	28.608	1.096	.8824E-06
22.908	1.160	.3696E-05	28.758	1.115	.1034E-05
23.058	1.077	.1744E-05	28.908	1.113	.9969E-06
23.208	1.013	.2837E-06	29.058	1.070	.5999E-06
23.358	1.085	.1834E-05	29.208	1.260	.2184E-05
23.508	1.108	.2264E-05	29.358	1.217	.1780E-05
23.658	1.071	.1463E-05	29.508	1.073	.5872E-06
23.808	1.095	.1912E-05	29.658	1.342	.2673E-05
23.958	1.152	.2963E-05	29.808	1.255	.1944E-05
24.108	1.132	.2520E-05	29.958	1.280	.2087E-05
24.258	1.157	.2924E-05	30.108	1.405	.2946E-05

Table A14. Lidar Data Taken on January 28, 1984, at GMT 2242–2254 Between 44.3°N, 69.9°W and 43.5°N, 70.6°W

Altitude, km	Scattering ratio	Scattering function, $(km\text{-}sr)^{-1}$	Altitude, km	Scattering ratio	Scattering function, $(km\text{-}sr)^{-1}$
8.908	1.015	.2977E-05	14.758	1.487	.3973E-04
9.058	1.054	.1082E-04	14.908	1.513	.4099E-04
9.208	1.106	.2051E-04	15.058	1.560	.4372E-04
9.358	1.152	.2879E-04	15.208	1.640	.4896E-04
9.508	1.185	.3409E-04	15.358	1.769	.5754E-04
9.658	1.208	.3736E-04	15.508	1.856	.6266E-04
9.808	1.236	.4138E-04	15.658	1.894	.6408E-04
9.956	1.260	.4444E-04	15.808	1.924	.6482E-04
10.108	1.285	.4749E-04	15.958	1.899	.6168E-04
10.258	1.326	.5316E-04	16.108	1.899	.6034E-04
10.408	1.368	.5864E-04	16.258	1.949	.6234E-04
10.558	1.392	.6091E-04	16.408	1.955	.6134E-04
10.708	1.410	.6228E-04	16.558	1.963	.6052E-04
10.858	1.442	.6554E-04	16.708	1.969	.5955E-04
11.008	1.464	.6731E-04	16.858	1.944	.5675E-04
11.158	1.477	.6748E-04	17.008	1.932	.5483E-04
11.308	1.500	.6917E-04	17.158	1.932	.5361E-04
11.458	1.539	.7273E-04	17.308	1.927	.5218E-04
11.608	1.556	.7336E-04	17.458	1.909	.5006E-04
11.758	1.543	.6986E-04	17.608	1.887	.4773E-04
11.908	1.500	.6286E-04	17.758	1.856	.4509E-04
12.058	1.470	.5763E-04	17.908	1.799	.4115E-04
12.208	1.476	.5704E-04	18.058	1.759	.3823E-04
12.358	1.481	.5624E-04	18.208	1.644	.3173E-04
12.508	1.476	.5435E-04	18.358	1.497	.2390E-04
12.658	1.500	.5575E-04	18.508	1.411	.1928E-04
12.808	1.555	.6040E-04	18.658	1.358	.1642E-04
12.958	1.626	.6653E-04	18.808	1.344	.1539E-04
13.108	1.673	.6980E-04	18.958	1.337	.1469E-04
13.258	1.709	.7180E-04	19.108	1.344	.1465E-04
13.408	1.765	.7571E-04	19.258	1.396	.1646E-04
13.558	1.776	.7524E-04	19.408	1.401	.1627E-04
13.708	1.706	.6693E-04	19.558	1.385	.1524E-04
13.858	1.627	.5821E-04	19.708	1.361	.1396E-04
14.008	1.578	.5247E-04	19.858	1.373	.1405E-04
14.158	1.578	.5139E-04	20.008	1.384	.1412E-04
14.308	1.509	.4431E-04	20.158	1.325	.1168E-04
14.458	1.486	.4135E-04	20.308	1.256	.8989E-05
14.608	1.472	.3936E-04	20.458	1.219	.7483E-05

Table A14. Concluded

Altitude, km	Scattering ratio	Scattering function, $(km\text{-}sr)^{-1}$	Altitude, km	Scattering ratio	Scattering function, $(km\text{-}sr)^{-1}$
20.608	1.206	.6878E-05	26.458	1.209	.2758E-05
20.758	1.182	.5942E-05	26.608	1.144	.1854E-05
20.908	1.186	.5934E-05	26.758	1.054	.6744E-06
21.058	1.177	.5533E-05	26.908	1.053	.6466E-06
21.208	1.181	.5507E-05	27.058	1.087	.1046E-05
21.358	1.195	.5809E-05	27.208	1.129	.1509E-05
21.508	1.181	.5262E-05	27.358	1.197	.2260E-05
21.658	1.154	.4383E-05	27.508	1.230	.2578E-05
21.808	1.150	.4166E-05	27.658	1.208	.2283E-05
21.958	1.163	.4424E-05	27.808	1.208	.2224E-05
22.108	1.151	.3996E-05	27.958	1.274	.2868E-05
22.258	1.096	.2477E-05	28.108	1.322	.3288E-05
22.408	1.106	.2689E-05	28.258	1.321	.3205E-05
22.558	1.126	.3099E-05	28.408	1.231	.2253E-05
22.708	1.099	.2377E-05	28.558	1.131	.1246E-05
22.858	1.091	.2137E-05	28.708	1.116	.1077E-05
23.008	1.088	.2028E-05	28.858	1.107	.9742E-06
23.158	1.089	.1997E-05	29.008	1.093	.8268E-06
23.308	1.084	.1844E-05	29.158	1.136	.1178E-05
23.458	1.076	.1621E-05	29.308	1.179	.1515E-05
23.608	1.057	.1186E-05	29.458	1.220	.1819E-05
23.758	1.030	.6121E-06	29.608	1.240	.1942E-05
23.908	1.029	.5697E-06	29.758	1.171	.1353E-05
24.058	1.044	.8627E-06	29.908	1.162	.1249E-05
24.208	1.073	.1385E-05	30.058	1.137	.1035E-05
24.358	1.087	.1612E-05	30.208	1.083	.6143E-06
24.508	1.077	.1388E-05	30.358	1.146	.1054E-05
24.658	1.059	.1038E-05	30.508	1.283	.1987E-05
24.808	.980	-.3459E-06	30.658	1.359	.2467E-05
24.958	.933	-.1134E-05			
25.108	.989	-.1884E-06			
25.258	1.040	.6440E-06			
25.408	1.078	.1213E-05			
25.558	1.053	.8048E-06			
25.708	.948	-.7760E-06			
25.858	.983	-.2406E-06			
26.008	1.141	.1998E-05			
26.158	1.201	.2783E-05			
26.308	1.206	.2785E-05			

Table A15. Lidar Data Taken on January 28, 1984, at GMT 2324–2349 Between 41.4°N, 72.1°W and 39.8°N, 73.8°W

Altitude, km	Scattering ratio	Scattering function, $(km\text{-}sr)^{-1}$	Altitude, km	Scattering ratio	Scattering function, $(km\text{-}sr)^{-1}$
8.008	1.047	.1067E-04	13.858	1.405	.3755E-04
8.158	1.229	.5137E-04	14.008	1.439	.3988E-04
8.308	1.427	.9413E-04	14.158	1.453	.4031E-04
8.458	1.662	.1433E-03	14.308	1.423	.3681E-04
8.608	2.004	.2135E-03	14.458	1.412	.3510E-04
8.758	2.340	.2801E-03	14.608	1.401	.3345E-04
8.908	2.589	.3240E-03	14.758	1.410	.3340E-04
9.058	2.725	.3428E-03	14.908	1.416	.3318E-04
9.208	2.878	.3641E-03	15.058	1.423	.3307E-04
9.358	3.048	.3870E-03	15.208	1.426	.3254E-04
9.508	2.624	.2992E-03	15.358	1.436	.3262E-04
9.658	1.746	.1340E-03	15.508	1.470	.3443E-04
9.808	1.292	.5111E-04	15.658	1.549	.3938E-04
9.958	1.195	.3328E-04	15.808	1.609	.4274E-04
10.108	1.136	.2264E-04	15.958	1.646	.4434E-04
10.258	1.168	.2732E-04	16.108	1.693	.4652E-04
10.408	1.196	.3127E-04	16.258	1.722	.4741E-04
10.558	1.223	.3466E-04	16.408	1.741	.4760E-04
10.708	1.239	.3629E-04	16.558	1.760	.4776E-04
10.858	1.257	.3815E-04	16.708	1.777	.4776E-04
11.008	1.274	.3969E-04	16.858	1.797	.4790E-04
11.158	1.277	.3922E-04	17.006	1.805	.4733E-04
11.308	1.261	.3616E-04	17.158	1.789	.4538E-04
11.458	1.232	.3139E-04	17.308	1.782	.4399E-04
11.608	1.187	.2470E-04	17.458	1.767	.4221E-04
11.758	1.120	.1545E-04	17.608	1.721	.3882E-04
11.908	1.064	.8024E-05	17.758	1.664	.3495E-04
12.058	1.060	.7379E-05	17.908	1.599	.3085E-04
12.208	1.102	.1218E-04	18.058	1.547	.2757E-04
12.358	1.150	.1751E-04	18.208	1.526	.2594E-04
12.508	1.175	.1992E-04	18.358	1.523	.2518E-04
12.658	1.191	.2124E-04	18.508	1.539	.2528E-04
12.808	1.214	.2326E-04	18.658	1.532	.2437E-04
12.958	1.247	.2627E-04	18.808	1.442	.1977E-04
13.108	1.292	.3028E-04	18.958	1.387	.1688E-04
13.258	1.317	.3208E-04	19.108	1.396	.1685E-04
13.408	1.331	.3275E-04	19.258	1.384	.1597E-04
13.558	1.348	.3372E-04	19.408	1.322	.1304E-04
13.708	1.367	.3481E-04	19.558	1.274	.1083E-04

Table A15. Concluded

Altitude, km	Scattering ratio	Scattering function, $(km\text{-}sr)^{-1}$	Altitude, km	Scattering ratio	Scattering function, $(km\text{-}sr)^{-1}$
19.708	1.214	.8252E-05	25.558	1.067	.1016E-05
19.858	1.172	.6476E-05	25.708	1.030	.4405E-06
20.008	1.164	.6030E-05	25.858	1.061	.8927E-06
20.158	1.143	.5137E-05	26.008	1.024	.3441E-06
20.308	1.140	.4916E-05	26.158	.961	-.5459E-06
20.458	1.157	.5373E-05	26.308	.971	-.3921E-06
20.608	1.180	.6019E-05	26.458	1.019	.2528E-06
20.758	1.172	.5605E-05	26.608	1.040	.5169E-06
20.908	1.157	.4996E-05	26.758	1.009	.1167E-06
21.058	1.158	.4939E-05	26.908	.973	-.3298E-06
21.208	1.121	.3675E-05	27.058	1.029	.3545E-06
21.358	1.071	.2125E-05	27.208	1.060	.7005E-06
21.508	1.048	.1389E-05	27.358	1.016	.1875E-06
21.658	1.039	.1106E-05	27.508	.991	-.9726E-07
21.808	1.045	.1238E-05	27.658	1.011	.1247E-06
21.958	1.024	.6639E-06	27.808	1.070	.7497E-06
22.108	1.027	.7111E-06	27.958	1.029	.3082E-06
22.258	1.045	.1171E-05	28.108	1.036	.3700E-06
22.408	1.024	.6006E-06	28.258	1.065	.6522E-06
22.558	.992	-.1954E-06	28.408	1.100	.9759E-06
22.708	1.002	.4889E-07	28.558	1.150	.1427E-05
22.858	1.001	.1925E-07	28.708	1.172	.1597E-05
23.008	.997	-.7065E-07	28.858	1.144	.1312E-05
23.158	1.018	.4007E-06	29.008	1.106	.9416E-06
23.308	1.024	.5210E-06	29.158	1.157	.1363E-05
23.458	.980	-.4269E-06	29.308	1.226	.1916E-05
23.608	.987	-.2817E-06	29.458	1.209	.1731E-05
23.758	1.009	.1827E-06	29.608	1.117	.9468E-06
23.908	1.019	.3842E-06	29.758	1.083	.6582E-06
24.058	1.034	.6691E-06	29.908	1.121	.9338E-06
24.208	.980	-.3713E-06	30.058	1.173	.1301E-05
24.358	.999	-.9283E-08	30.208	1.183	.1346E-05
24.508	1.077	.1388E-05	30.358	1.237	.1708E-05
24.658	1.135	.2388E-05	30.508	1.352	.2474E-05
24.808	1.139	.2387E-05	30.658	1.366	.2513E-05
24.958	1.107	.1803E-05			
25.108	1.119	.1957E-05			
25.258	1.113	.1810E-05			
25.408	1.103	.1604E-05			

References

1. McCormick, M. Patrick; and Osborn, M. T.: *Airborne Lidar Measurements of El Chichon Stratospheric Aerosols—July 1982.* NASA RP-1166, 1986.
2. McCormick, M. Patrick; and Osborn, M. T.: *Airborne Lidar Measurements of El Chichon Stratospheric Aerosols—October 1982 to November 1982.* NASA RP-1136, 1985.
3. McCormick, M. Patrick; and Osborn, M. T.: *Airborne Lidar Measurements of El Chichon Stratospheric Aerosols—January 1983 to February 1983.* NASA RP-1148, 1985.
4. McCormick, M. Patrick; and Osborn, M. T.: *Airborne Lidar Measurements of El Chichon Stratospheric Aerosols—May 1983.* NASA RP-1172, 1986.
5. McCormick, M. P.; Hamill, Patrick; Pepin, T. J.; Chu, W. P.; Swissler, T. J.; and McMaster, L. R.: Satellite Studies of the Stratospheric Aerosol. *Bull. American Meteorol. Soc.*, vol. 60, no. 9, Sept. 1979, pp. 1038–1046.
6. McCormick, M. P.; Hamill, Patrick; and Farrukh, U. O.: Characteristics of Polar Stratospheric Clouds as Observed by SAM II, SAGE, and Lidar. *J. Meteorol. Soc. Japan,* vol. 63, no. 2, Apr. 1985, pp. 267–276.
7. Kent, G. S.; Poole, L. R.; and McCormick, M. P.: Characteristics of Arctic Polar Stratospheric Clouds as Measured by Airborne Lidar. *J. Atmos. Sci.*, vol. 43, no. 20, Oct. 15, 1986, pp. 2149–2161.
8. Russell, Philip B.; Swissler, Thomas J.; and McCormick, M. Patrick: Methodology for Error Analysis and Simulation of Lidar Aerosol Measurements. *Appl. Opt.*, vol. 18, no. 22, Nov. 15, 1979, pp. 3783–3797.
9. McCormick, M. P.; Swissler, T. J.; Chu, W. P.; and Fuller, W. H., Jr.: Post-Volcanic Stratospheric Aerosol Decay as Measured by Lidar. *J. Atmos. Sci.*, vol. 35, no. 7, July 1978, pp. 1296–1303.
10. McCormick, M. P.; Swissler, T. J.; Fuller, W. H.; Hunt, W. H.; and Osborn, M. T.: Airborne and Ground-Based Lidar Measurements of the El Chichon Stratospheric Aerosol From 90°N to 56°S. *Geofis. Int.*, vol. 23, no. 2, Apr. 1984, pp. 187–221.

Standard Bibliographic Page

1. Report No.	2. Government Accession No.	3. Recipient's Catalog No.
NASA RP-1175		

4. Title and Subtitle	5. Report Date
Airborne Lidar Measurements of El Chichon Stratospheric Aerosols—January 1984	April 1987
	6. Performing Organization Code
7. Author(s)	8. Performing Organization Report No.
M. Patrick McCormick and M. T. Osborn	L-16234
9. Performing Organization Name and Address	10. Work Unit No.
NASA Langley Research Center Hampton, VA 23665-5225	672-21-14-70
	11. Contract or Grant No.
12. Sponsoring Agency Name and Address	13. Type of Report and Period Covered
National Aeronautics and Space Administration Washington, DC 20546-0001	Reference Publication
	14. Sponsoring Agency Code

15. Supplementary Notes

M. Patrick McCormick: Langley Research Center, Hampton, Virginia.
M. T. Osborn: ST Systems Corporation (STX), Hampton, Virginia.
Previous reports in this series: NASA RP-1166, NASA RP-1136, NASA RP-1148, NASA RP-1172.

16. Abstract

A NASA Electra airplane, outfitted with a lidar system, was flown in January 1984 between the latitudes of 38°N and 90°N. One of the primary purposes of this mission was to determine the spatial distribution and aerosol characteristics of the El Chichon-produced stratospheric material. This report presents lidar data from that portion of the flight mission between 38°N and 77°N. Representative profiles of lidar backscatter ratio, a plot of the integrated backscattering function versus latitude, and contours of backscatter mixing ratio versus altitude and latitude are given. In addition, tables containing numerical values of the backscatter ratio and backscattering function versus altitude are supplied for each profile. These data clearly show that material produced by the El Chichon eruptions of late March–early April 1982 had spread throughout the latitudes covered by this mission, and that the most massive portion of the material resided north of 55°N and was concentrated below 17 km in a layer that peaked at 13 to 15 km. In this latitude region, peak backscatter ratios at a wavelength of 0.6943 μm were approximately 3 and the peak integrated backscattering function was about 15×10^{-4} sr^{-1}, corresponding to a peak optical depth of approximately 0.07. This report presents the results of this mission in a ready-to-use format for atmospheric and climatic studies.

17. Key Words (Suggested by Authors(s))	18. Distribution Statement
Lidar Volcanoes El Chichon Stratospheric aerosols	Unclassified—Unlimited Subject Category 46

19. Security Classif.(of this report)	20. Security Classif.(of this page)	21. No. of Pages	22. Price
Unclassified	Unclassified	48	A03

For sale by the National Technical Information Service, Springfield, Virginia 22161

NASA-Langley, 1987